HHS Public Access

Author manuscript

Nat Immunol. Author manuscript; available in PMC 2024 October 16.

Published in final edited form as:

Nat Immunol. 2023 December ; 24(12): 2121–2134. doi:10.1038/s41590-023-01663-2.

CD3ζ ITAMs enable ligand discrimination and antagonism by inhibiting TCR signaling in response to low-affinity peptides

Guillaume Gaud[1], **Sooraj Achar**[2,3,13], **François X. P. Bourassa**[4,5,13], **John Davies**[6,11,13], **Teri Hatzihristidis**[1], **Seeyoung Choi**[1], **Taisuke Kondo**[7], **Selamawit Gossa**[8], **Jan Lee**[1], **Paul Juneau**[9], **Naomi Taylor**[7], **Christian S. Hinrichs**[6,12], **Dorian B. McGavern**[8], **Paul François**[4,10], **Grégoire Altan-Bonnet**[2], **Paul E. Love**[1,✉]

[1]Hematopoiesis and Lymphocyte Biology Section, Eunice Kennedy Shriver, National Institute of Child Health and Human Development, Bethesda, MD, USA.

[2]Immunodynamics Section, Laboratory of Integrative Cancer Immunology, Center for Cancer Research, National Cancer Institute, Bethesda, MD, USA.

[3]Nuffield Department of Orthopaedics, Rheumatology and Musculoskeletal Sciences, Kennedy Institute of Rheumatology, University of Oxford, Oxford, UK.

[4]Département de Biochimie et Médecine Moléculaire, Université de Montréal, Montréal, Quebec, Canada.

[5]Department of Physics, McGill University, Montréal QC, Canada.

[6]Genitourinary Malignancies Branch, Center for Cancer Research, National Cancer Institute, Bethesda, MD, USA.

✉**Correspondence and requests for materials** should be addressed to Paul E. Love lovep@mail.nih.gov.

Author contributions

G.G., J.D., S.A., F.X.P.B., C.S.H., P.F., D.B.M., P.J., N.T., G.A.-B. and P.E.L. conceptualized the study. G.G., J.D., S.A., F.X.P.B., P.F., D.B.M., G.A.-B. and P.E.L. devised the methodology. G.G., J.D., S.A., F.X.P.B., T.H., S.C., T.K., S.G. and J.L. carried out experiments. G.G., C.S.H., P.F., D.B.M., G.A.-B. and P.E.L. acquired the funding. G.G., G.A.-B. and P.E.L. administered the project. C.S.H., P.F., D.B.M., G.A.-B. and P.E.L. supervised the study. G.G. and P.E.L. wrote the original draft. G.G., J.D., S.A., F.X.P.B., C.S.H., P.J., P.F., N.T., G.A.-B. and P.E.L. reviewed and edited the draft.

Online content

Any methods, additional references, Nature Portfolio reporting summaries, source data, extended data, supplementary information, acknowledgements, peer review information; details of author contributions and competing interests; and statements of data and code availability are available at https://doi.org/10.1038/s41590-023-01663-2.

Reporting summary

Further information on research design is available in the Nature Portfolio Reporting Summary linked to this article.

Competing interests

G.G., J.D., C.S.H. and P.E.L. are inventors on an NIH patent using ITAM-mutated CD3ζ to enhance the function of cytotoxic T cells and other immune cells; Patent #: 63/113,428. The remaining authors declare no competing interests.

Additional information

Extended data is available for this paper at https://doi.org/10.1038/s41590-023-01663-2.

Supplementary information The online version contains supplementary material available at https://doi.org/10.1038/s41590-023-01663-2.

Peer review information *Nature Immunology* thanks Stephen Jameson and the other, anonymous, reviewer(s) for their contribution to the peer review of this work. Peer reviewer reports are available. Primary Handling Editor: S. Houston in collaboration with the rest of the *Nature Immunology* editorial team.

[7]Pediatric Oncology Branch, Center for Cancer Research, National Cancer Institute, Bethesda, MD, USA.

[8]Viral Immunology & Intravital Imaging Section, National Institute of Neurological Disorders and Stroke, Bethesda, MD, USA.

[9]National Institutes of Health Library, Office of Research Services, National Institutes of Health, Bethesda, MD, USA.

[10]Mila Québec, Montréal, Quebec, Canada.

[11]Present address: Department of Safety Assessment, Genentech, Inc., San Francisco, CA, USA.

[12]Present address: Duncan and Nancy MacMillan Cancer Immunology and Metabolism Center of Excellence, Rutgers Cancer Institute of New Jersey, New Brunswick, NJ, USA.

[13]These authors contributed equally and are listed alphabetically: Sooraj Achar, François X. P. Bourassa, John Davies.

Abstract

The T cell antigen receptor (TCR) contains ten immunoreceptor tyrosine-based activation motif (ITAM) signaling sequences distributed within six CD3 subunits; however, the reason for such structural complexity and multiplicity is unclear. Here we evaluated the effect of inactivating the three CD3ζ chain ITAMs on TCR signaling and T cell effector responses using a conditional ‘switch’ mouse model. Unexpectedly, we found that T cells expressing TCRs containing inactivated (non-signaling) CD3ζ ITAMs (6F-CD3ζ) exhibited reduced ability to discriminate between low- and high-affinity ligands, resulting in enhanced signaling and cytokine responses to low-affinity ligands because of a previously undetected inhibitory function of CD3ζ ITAMs. Also, 6F-CD3ζ TCRs were refractory to antagonism, as predicted by a new in silico adaptive kinetic proofreading model that revises the role of ITAM multiplicity in TCR signaling. Finally, T cells expressing 6F-CD3ζ displayed enhanced cytolytic activity against solid tumors expressing low-affinity ligands, identifying a new counterintuitive approach to TCR-mediated cancer immunotherapy.

The T cell antigen receptor (TCR), which performs a singular and essential role in adaptive immunity by conferring antigen recognition to T cells and by initiating signaling responses that lead to proliferation, cytokine production and cytolytic activity, exhibits exquisite ligand sensitivity and a remarkable capacity for ligand discrimination[1–3]. The clonotype-specific TCRα and TCRβ subunits are responsible for antigen peptide–major histocompatibility complex (MHC) binding but lack signal transducing capability. TCRα/TCRβ heterodimers associate non-covalently with multiple invariant CD3 subunits (the γ, δ, ε and ζ chains) that contain one or more di-tyrosine signaling motifs termed immunoreceptor tyrosine-based activation motifs (ITAMs)[4,5]. Phosphorylation of both ITAM tyrosines by the tyrosine-protein kinase Lck (LCK) is one of the first steps after TCR engagement by peptide–MHC that results in the recruitment and activation of the tyrosine-protein kinase ZAP-70 (ZAP-70) and the subsequent activation of multiple downstream signaling pathways[6].

The TCR contains a total of ten ITAMs, unique among immune receptors, yet the reason for this striking ITAM multiplicity has not been fully elucidated despite over three decades of research[7–9]. The presence of at least one ITAM is necessary and sufficient for the initiation of TCR signal transduction, and none of the TCR ITAMs are essential for T cell development or for T cell effector functions, suggesting substantial functional redundancy among TCR ITAMs[8–10]. In some but not all experimental contexts, multiple TCR ITAMs operate additively by amplifying the TCR signaling response or by increasing the probability of T cell activation[9,11–13]; however, the importance of this function for T cell effector responses is unclear[14–16].

Previous studies suggested a potential inhibitory function for CD3ζ ITAM tyrosines under certain conditions; however, this activity has not been clearly or consistently defined or demonstrated in the context of the TCR[17]. A role for CD3ζ ITAMs in TCR antagonism was suggested from the observation that engagement of the TCR by antagonist ligands leads to incomplete phosphorylation of CD3ζ ITAM tyrosines[18–20]. Nevertheless, the precise role of CD3ζ ITAMs in TCR antagonism is unresolved, with some studies[19,21] but not others[22–25] correlating antagonism with incomplete or altered CD3ζ ITAM phosphorylation, and with conflicting results concerning whether antagonism is associated with and mediated by 'inhibitory' TCR signals that can act in *trans*[17,25–27].

Recent efforts in synthetic immunology include studies aimed at endowing T cells with new immunotherapeutic functions for cancer treatment[28]. Chimeric antigen receptors (CARs) have been designed to combine the specificity of antibody recognition of antigens with the signaling motifs from CD3ζ ITAMs and costimulatory molecules[29]. TCR-based strategies for immunotherapy are also being actively pursued[30]. One approach to increase the functionality of both CARs and TCRs has involved attempts to optimize signaling by modifying the type or number of ITAMs contained within these receptors[11,31,32]. However, 'fine-tuning' of T cell responses for therapeutic purposes will require a more fundamental understanding of the functional role of multiplexed ITAM tyrosine phosphorylation in the TCR, especially when exploring the efficacy of different ITAM configurations.

To enable a more precise analysis of the role of ITAM multiplicity in TCR signaling responses, we generated a 'knock-in CD3ζ-switch' mouse model in which a mutant CD3ζ chain (designated 6F, where all six of the CD3ζ ITAM tyrosines (Y) are replaced by a phenylalanine (F) rendering CD3ζ signaling incompetent) can be substituted for the wild-type (WT) (6Y) CD3ζ chain in mature postselection T cells by Cre-mediated recombination at the endogenous CD3ζ locus[14]. Consistent with previous results, TCRs that contained ITAM mutant 6F-CD3ζ subunits (comprising only the four ITAMs contributed by the CD3γ, CD3δ, and two ε chains) exhibited reduced signaling responses to antibody cross-linking or high-affinity ligands reflecting an amplifying function for TCR ITAM multiplicity[9]. Unexpectedly, we found that 6F-CD3ζ TCRs displayed enhanced signaling responses to low-affinity ligands due to the loss of a previously unidentified inhibitory function of CD3ζ ITAMs mediated by the protein-tyrosine phosphatase SHP1 (PTPN6). A latent space (LS) analysis confirmed that patterns of ligand recognition are qualitatively different for 6Y-CD3ζ and 6F-CD3ζ TCRs, the latter exhibiting impaired ligand discrimination and a resistance to antagonism. With a new mathematical model

incorporating these insights, we predicted several antagonist responses that were confirmed experimentally, demonstrating that the large number of phosphorylations afforded by the ten TCR ITAMs not only quantitatively enhance downstream signaling, but also qualitatively generate more functionality. Finally, we performed initial proof-of-concept experiments demonstrating that *6F-CD3ζ* T cells exhibit enhanced cytolytic activity against solid tumors expressing low-affinity antigens. Together, these results call for revision of the current paradigm of the role of CD3ζ ITAMs in TCR signaling and identify a promising new approach for improving the efficacy of TCR-mediated tumor immunotherapy.

Results

Inactivation of CD3ζ ITAMs enhances some TCR signaling responses

We generated three Cre transgenic lines in *CD3ζ 6Y/6Y* 'knock-in' mice (Fig. 1a) collectively designated *6F(i)* for 'induced', where the switch from expression of FLAG-tagged WT 6Y-CD3ζ to Myc-tagged mutant 6F-CD3ζ chain was or could be induced in mature postselection T cells using either (1) *Ert2-Cre* where the *6Y* to *6F* switch could be induced by tamoxifen[33], (2) *dLck-Cre*, where the 6Y to *6F* switch occurs in $CD4^+CD8^-$ and $CD4^-CD8^+$ thymocytes after positive selection[34] or (3) *OX40-Cre*, where the *6Y* to *6F* switch is induced in activated $CD4^+$ and $CD8^+$ T cells[35]. Stimulation of germline *6F/6F (6F)*, *dLck-Cre 6Y/6Y (6F(i))*, or tamoxifen-induced *Ert2-Cre 6Y/6Y (6F(i))* $CD8^+$ T cells with anti-CD3 alone or in combination with anti-CD28 elicited reduced activation and proliferation responses compared to control *6Y/6Y (6Y)* $CD8^+$ T cells (Fig. 1b–e), which is consistent with previous results suggesting a role for CD3ζ ITAMs in TCR signal amplification[9,36]. To evaluate in vivo antigen-mediated TCR responses, we infected age and sex-matched germline *6Y*, germline *6F* and *OX40-Cre 6Y/6Y (6F(i))* mice with lymphocytic choriomeningitis virus (LCMV) Armstrong and assessed viral antigen-specific T cell responses 8 days after LCMV infection. Unexpectedly, the response of both germline *6F* and induced *6F(i)* $CD8^+$ T cells to NP396 and GP33, and the response of *6F* and *6F(i)* $CD4^+$ T cells to GP61 was superior to that of *6Y* T cells (Fig. 1f). The enhanced response of germline *6F* T cells could be due to changes in the expression of signaling effectors or an altered TCRα and TCRβ repertoire caused by preselection reduction in functional TCR ITAMs as documented previously[14,15]. However, because *6F(i)* T cells arise from thymocytes that are positively selected by TCRs that contain WT 6Y-CD3ζ and their phenotype closely resembles that of *6Y* mice (Extended Data Fig. 1), their enhanced response to some LCMV-encoded ligands cannot be explained by thymocyte selection-associated compensatory changes. These results revealed that the effect of CD3ζ ITAM inactivation on TCR-mediated cytokine responses is variable depending on the nature (affinity) of the TCR and peptide–MHC interaction, suggesting that CD3ζ ITAMs may be inhibitory under certain conditions.

Enhanced activation of *6F(i)* T cells by low-affinity ligands

As strong artificial stimulation by antibody-mediated TCR cross-linking could be masking subtle alterations in TCR signaling, we used a more physiological system of antigen stimulation, the MHC class I-restricted OTI TCR transgenic model. OTI TCR transgenic $CD8^+$ T cells express defined TCRα and TCRβ subunits specific for an avian ovalbumin

(OVA)-derived peptide: SIINFEKL (OVA/N4)[37]. We first confirmed that the phenotypes of *OTI-6Y* and *OTI-6F(i)* thymocytes and T cells were similar (Extended Data Fig. 2a–e). Next, we used an automated robotic instrument[38] to monitor cytokine expression in real time using *OTI* $CD8^+$ T cells stimulated in vitro with antigen-presenting cells (APCs) pulsed with agonist peptide N4 (OVA) or N4-derived altered peptide ligands (APLs) of varying affinity for the OTI TCR spanning a range of ligand potency (functional avidity) of more than 50,000-fold[37,39] (Fig. 2a). In these experiments, *dLck-Cre OTI-6F(i)* $CD8^+$ T cells unexpectedly produced more interleukin-2 (IL-2) when stimulated with the moderate- to low-affinity peptides Q4, T4, V4 and G4 than did *OTI-6Y* $CD8^+$ T cells, whereas no T cells reacted to the lowest-affinity 'null' peptide E1 (Fig. 2b,c). A similar overall trend was observed with induced expression of the activation markers CD44, CD25 and CD69 (Extended Data Fig. 2f,g) and with antigen-induced production of interleukin-6 (IL-6), interferon-γ (IFNγ) and tumor necrosis factor (TNF), although the sensitivity varied for each cytokine, indicating different TCR signal strength requirements and kinetics for individual cytokine responses (Fig. 2c and Extended Data Fig. 3a–d). This phenotype was not specific to the *dLck-Cre OTI-6F(i)* model because similar results were obtained with *Ert2-Cre OTI-6F(i)* $CD8^+$ T cells (Extended Data Fig. 3e). The superior response of *OTI-6F(i)* T cells to low-affinity ligands could in some cases be partially mitigated by increasing the ligand concentration and therefore the avidity of the TCR and peptide–MHC interaction (Extended Data Fig. 4a,b). *OTI-6F(i)* $CD8^+$ T cells proliferated less than *OTI-6Y* $CD8^+$ T cells when stimulated in vitro with anti-CD3 plus anti-CD28 but proliferated more when stimulated in vitro with low-affinity peptides (Extended Data Figs. 2f and 4c) or when coinjected into B6 hosts that were subsequently challenged with low-affinity peptide-pulsed APCs (Fig. 2d). Together, these results suggested a dual, antinomic (activating or inhibitory) role for CD3ζ ITAMs in TCR signaling depending on the affinity (strength) of the TCR-ligand interaction.

We next tested whether *6F(i)* T cells could be activated by very-low-affinity self-peptides. A peptide derived from β-catenin (RTYTYEKL, Catnb), promotes positive selection of OTI thymocytes but it is incapable of activating mature OTI T cells[40]. *OTI-6F(i)* $CD8^+$ T cells did not respond to Catnb either as naive cells (Fig. 2e) or after preactivation with the N4 agonist peptide (Fig. 2f). *6Y* T cells and *6F(i)* T cells proliferated to the same extent in T or B cell-deficient *Rag2*$^{-/-}$ hosts (Fig. 2g) and in competitive bone marrow chimeras, where the ratio and naive and memory surface phenotype of WT +/+ and *6F(i)* $CD4^+$ and $CD8^+$ T cells was unchanged after in vivo tamoxifen-induced *6Y-6F* switching (Fig. 2h). Collectively, these findings indicated that although expression of 6F-CD3ζ increases TCR sensitivity to low-affinity ligands, it does not make TCRs overtly self-reactive, which is consistent with the absence of autoimmune disease in germline *6F* mice[14].

Enhanced *6F(i)* TCR signaling responses to low-affinity ligands

OTI-6F(i) $CD8^+$ T cells expressed significantly more interferon regulatory factor 4 (IRF4), which has been shown to quantitatively reflect TCR signal intensity[41], than *OTI-6Y* $CD8^+$ T cells in response to the low-affinity G4 peptide but not when stimulated with the high-affinity N4 peptide (Fig. 3a). In addition, phosphorylation of the TCR-proximal signaling proteins ZAP-70, linker for activation of T cells (LAT) and extracellular signal-regulated

kinase (ERK) was increased in *OTI-6F(i)* $CD8^+$ T cells compared to *OTI-6Y* $CD8^+$ T cells in response to stimulation with low-affinity peptides (Fig. 3b and Extended Data Fig. 4d) or low affinity peptide tetramers (Fig. 3c and Extended Data Fig. 4e). Moreover, low-affinity OVA-derived peptides elicited stronger calcium flux responses from *OTI-6F(i)* $CD8^+$ T cells compared with *OTI-6Y* $CD8^+$ T cells (Fig. 3d). Indeed, stimulation with the lowest-affinity peptide tetramers (T4 and G4) induced calcium responses from *OTI-6F(i)* $CD8^+$ T cells but not from *OTI-6Y* $CD8^+$ T cells, whereas neither were responsive to the self-peptide Catnb (Fig. 3d).

CD3ζ-*6F(i)* T cells exhibit impaired ligand discrimination

We next evaluated if inactivation of CD3ζ ITAMs affects TCR ligand discrimination. *OTI-6F(i)* TCRs generated fewer distinct functional responses to OVA-APLs of varying affinity than *OTI-6Y* TCRs (Fig. 4a). Reduced ligand discrimination was most apparent with IFNγ and TNF responses (Fig. 4b), where *OTI-6F(i)* T cells exhibited enhanced responses to low-affinity ligands but reduced responses to high-affinity ligands, which is consistent with the data in Figs. 1–3 and previous results[9]. Impaired ligand discrimination was also observed with germline *OTI-6F* $CD8^+$ T cells, indicating that this is an intrinsic property of 6F-CD3ζ that is not affected by potential compensatory changes imposed during positive selection (Extended Data Fig. 5). We quantified the differences in the cytokine responses of *OTI-6Y* and *OTI-6F(i)* T cells by computing the mutual information (MI)[42,43] between cytokine outputs and antigen. WT *OT-6Y* TCRs readily discriminated 3–4 classes of antigen (MI approximately equal to 2 bits), while for IFNγ and TNF, *OTI-6F(i)* TCRs discriminated fewer than three classes of antigen (MI < 2 bits) (Fig. 4c), in some instances (for example, IFNγ; Fig. 4b) approximating an 'all-or-nothing' response. Reduced ligand discrimination was observed with both naive (Fig. 4b) and antigen restimulated blast (Extended Data Fig. 6a–c) *OTI-6F(i)* $CD8^+$ T cells. However, at low antigen doses (10^{-9} M), *OTI-6F(i)* and *OTI 6Y* $CD8^+$ T cells demonstrated comparable ligand discrimination, reflecting the balance between a reduced activation signal triggered by low doses of antigen in both *OTI-6Y* and *OTI- 6F(i)* T cells, and the enhanced response of *OTI-6F(i)* T cells to low-affinity ligands (Extended Data Fig. 6d–f).

We next applied a machine learning approach to obtain a simplified representation of antigen discrimination by the TCR using a process termed 'antigen encoding' (Fig. 4d)[38]. The projected cytokine time trajectories for *OTI-6Y* $CD8^+$ T cells in the LS (Fig. 4e, left) were qualitatively similar to those generated with WT-OTI $CD8^+$ T cells in our previous study[38]. However, two key differences were observed with *OTI-6F(i)* trajectories (Fig. 4e, right) that could be resolved by plotting the LS variables (LS_1 and LS_2) 36 h after activation (Fig. 4f). LS_1 increased monotonically with antigen affinity for both *OTI-6Y* and *OTI-6F(i)* T cells, with *OTI-6F(i)* T cells displaying enhanced sensitivity to all ligands except N4 (Fig. 4f, left). However, the second S coordinate, LS_2, revealed a qualitative discrepancy between *OTI-6Y* and *OTI-6F(i)* T cells, (Fig. 4f, right). WT *OTI-6Y* T cells exhibited a non-monotonic dependency for LS_2 as a function of antigen quality, while *OTI-6F(i)* T cells generated a simpler monotonic curve (Fig. 4f, right).

Non-monotonicity of LS_2 was previously hypothesized to indicate the activation of a negative feedback response in TCR signaling based on the adaptive kinetic proofreading (KPR) model for TCR antigen discrimination[38,44] that was predicted to be mediated by the tyrosine phosphatase SHP1 (refs. 3,45). This finding prompted us to investigate the recruitment of SHP1 to *6Y* and *6F(i)* TCRs.

6F TCRs do not retain or recruit SHP1 after TCR engagement

The tyrosine kinase ZAP-70 is bound to incompletely phosphorylated (p21) CD3ζ in un-activated ex vivo T cells; however, this pool of TCR-associated ZAP-70 is inactive[46,47]. As expected, tyrosine phosphorylated p21 CD3ζ was detected in unstimulated ex vivo and activated *OTI-6Y* $CD8^+$ T cells but not in *OTI-6F(i)* $CD8^+$ T cells (Figs. 1e, 3c and 5a). Consistent with previous results[13], CD3γ, CD3δ and CD3ε ITAMs were more strongly tyrosine phosphorylated in antigen-stimulated *OTI-6F(i)* $CD8^+$ T cells (Figs. 3c and 5a). ZAP-70 was not associated with CD3ζ in unstimulated *OTI-6F(i)* TCRs (Fig. 5b,c). However, ZAP-70 was recruited to both *OTI-6Y* and *OTI-6F(i)* TCRs after stimulation with low-affinity or high-affinity ligands (Fig. 5d), and notably, *OTI-6F(i)* TCRs were associated with more activated (Y319-phosphorylated) ZAP-70 (pZAP-70) than *OTI-6Y* TCRs (Fig. 5e,f). Whereas most of the pZAP-70 was associated with phosphorylated CD3ζ in *OTI-6Y* T cells after stimulation by low-affinity or high-affinity ligands, pZAP-70 was instead bound to phosphorylated CD3γ, CD3δ and CD3ε in antigen-stimulated *OTI-6F* T cells (Fig. 5g).

Engagement of the TCR by antagonist ligands results in partial (mono)phosphorylation of CD3-ζ ITAMs and this configuration has been speculated to inhibit T cell activation[18,19]. TCR stimulation by antagonists or weak agonists can also result in the recruitment of SHP1 (PTPN6), a tyrosine phosphatase that directly dephosphorylates ZAP-70, CD3 ITAMs and LCK, although the mechanism of SHP1 recruitment to the immune synapse and its possible dependence on phosphorylated ITAMs is controversial[25,45,48]. SHP1 was immunoprecipitated with the TCR in unstimulated naive *OTI-6Y* and *OTI-6F(i)* $CD8^+$ T cells (Fig. 5h,i). However, after TCR engagement by either low-affinity or high-affinity ligands, SHP1 was associated with *OTI-6Y* TCRs but not with *OTI-6F* TCRs, indicating that SHP1 is selectively recruited to (or retained by) phosphorylated CD3ζ ITAMs after ligand stimulation, resulting in SHP1-mediated inhibition of TCR signaling.

6F-CD3ζ TCRs are less susceptible to antagonism

A key prediction of the adaptive KPR model of antigen discrimination is the existence of antagonism[49,50]. Reduced recruitment or retention of SHP1 to *OTI-6F* TCRs after peptide stimulation suggested that *6F(i)* T cells might be less sensitive to antagonism. To test this hypothesis, we cultured naive *OTI-6Y* and *OTI-6F(i)* $CD8^+$ T cells with APC pulsed with 10^{-11} M high-affinity N4 peptide alone or in combination with 10^{-6} M low-affinity OVA-APL peptide V4 (Fig. 6a). Whereas N4 agonist stimulation of *OTI-6Y* T cells was strongly antagonized by V4 peptide, V4 failed to antagonize *OTI-6F(i)* T cells and notably even synergized with N4 so that N4 + V4 stimulation resulted in increased IL-2 secretion compared to stimulation with N4 peptide alone (Fig. 6a). Focusing the analysis on a single time point (18 h; Fig. 6b) revealed that *OTI-6Y* T cells were antagonized tenfold by V4 peptide whereas the *OTI-6F(i)* T cell response was enhanced by a factor of three (Fig. 6b,c).

This metric could be assessed at each individual time point over the 72-h assay (Fig. 6d) and averaged (Fig. 6e) to compare the overall responses of *OTI-6F(i)* versus *OTI-6Y* T cells.

V4 was a strict antagonist for *OTI-6Y* TCRs over a range of 10^{-6} M to 10^{-9} M (Fig. 6f,g). In contrast, for *OTI-6F(i)* TCRs, V4 functioned as a co-agonist with N4 at higher concentrations (10^{-6} M to 10^{-7} M), whereas at lower concentrations (10^{-8} M to 10^{-9} M) V4 functioned as an antagonist of N4; however, the degree of antagonism was always much less for *OTI-6F(i)* TCRs than for *OTI-6Y* TCRs at the same concentration of V4 (Fig. 6f,g). A similar relative effect on antagonism was observed with the low-affinity partial agonist G4, which functioned as an antagonist of N4 for both *OTI-6F(i)* and *OTI-6Y* TCRs, while the null peptide E1 failed to act as an antagonist of N4 for either TCR (Fig. 6g). Under conditions where a peptide functioned as a co-agonist for both *OTI-6F(i)* and *OTI-6Y* TCRs (for example, agonist Q4, co-agonist V4) the enhancing effect of 6F-CD3ζ on TCR signaling was also observed and titration of the agonist peptide revealed a concentration dependence (Fig. 6h). Together, these results indicate that 6F-CD3ζ can have both quantitative and qualitative effects on TCR antagonism that are dependent on antigen affinity and concentration; however, overall, under identical experimental conditions, *OTI-6F(i)* TCRs are consistently less susceptible to antagonism than *OTI-6Y* TCRs.

A new model of KPR with negative feedback

To explain the experimental results obtained with *OTI-6F(i)* T cells, we expanded our adaptive KPR model and compared two schemes with either a small number of proofreading steps (6F-CD3ζ TCRs) or a larger number of proofreading steps (6Y-CD3ζ TCRs). Importantly, we incorporated the observed difference in SHP1 recruitment (Fig. 5h,i) by lowering SHP1 recruitment for *6F(i)* TCRs with fewer proofreading steps (Fig. 7a and Supplementary Information). Such tuning of the model was experimentally validated by comparing dose–response curves for each antigen (Fig. 7b).

We also tested our new model with predictions for mixtures of agonist and antagonist ligands that can be achieved experimentally. The model accurately predicted a non-monotonicity of antagonism depending on the affinity of the antagonist ligand, with the null peptide (E1) not impacting the response, the very-low-affinity ligand (G4) antagonizing the response and the low-affinity partial agonist (V4) either antagonizing or enhancing the response of 6F CD3ζ TCRs (Fig. 7c). The model also accurately predicted that the 6F CD3ζ TCR, owing to its limited negative feedback, would be less prone to antagonism compared to the 6Y CD3ζ TCR (Fig. 7c). Second, we verified that our model could accurately predict the 6Y TCR and 6F TCR response for two agonist ligands (one strong: N4; one medium: Q4) at varied doses including the distinct patterns of antagonism or enhancement for *OTI-6Y* and *OTI-6F(i)* T cells (Fig. 7d). Finally, the model predicted that antagonist peptides would have different antagonist properties depending on the agonist dose, with stronger antagonism for the 6Y CD3ζ TCR and delayed feedback for the 6F CD3ζ TCR (Fig. 7e). Notably, we also demonstrated experimentally, and explained theoretically, how the differential impact of the negative feedback is best measured at low doses of agonist antigen, where differences in antagonistic properties between 6Y CD3ζ TCRs and 6F CD3ζ TCRs for different ligands are the most stringent (Fig. 7e). Collectively, our mathematical model

accurately predicted and our experimental results validated that WT 'signaling-competent' 6Y CD3ζ is critical to enforce a proximal negative feedback which is required for TCR ligand discrimination and antagonism.

Enhanced tumor cytotoxicity of *6F(i)* T cells

The enhanced signaling response of OTI-6F(i) TCRs to low-affinity ligands raised the possibility that this property could be employed to improve TCR-mediated T cell control of tumor growth, particularly in light of the observation that most tumor-associated antigens bind with much lower affinity to their cognate TCRs than foreign pathogen-derived antigens[51,52]. *OTI-6Y* and *OTI-6F(i)* $CD8^+$ T cells exhibited a similar $CD62L^-CD44^+CD5^{hi}$ phenotype and expressed similar levels of surface TCR after in vitro activation and expansion induced by N4 peptide (Extended Data Fig. 7a,b). However, *OTI-6F(i)* $CD8^+$ T cells displayed a lower threshold of activation when rechallenged with low-affinity or medium-affinity antigens (Extended Data Fig. 7c,d).

We first conducted in vitro killing experiments using B16-F10 murine melanoma cell lines engineered to express OVA-APLs. *OTI-6F(i)* $CD8^+$ T cells exhibited markedly better in vitro tumoricidal activity than *OTI-6Y* $CD8^+$ T cells against B16-F10 melanomas that expressed medium-affinity or low-affinity ligands (Fig. 8a and Extended Data Fig. 7e). *OTI-6F(i)* $CD8^+$ T cells exhibited similar or slightly less ability to kill B16-F10-N4 melanoma cells compared with *OTI-6Y* $CD8^+$ T cells (Fig. 8a and Extended Data Fig. 7e). Consistent with the in vitro results, *OTI-6F(i)* T cells were superior to *OTI-6Y* T cells in their ability to control the growth of B16-F10 melanomas expressing the low-affinity OTI ligand V4, but not the high-affinity ligand, N4 (Fig. 8b and Extended Data Fig. 8a). *OTI* germline *6F* $CD8^+$ T cells also extended the survival of B16-F10-V4 tumor-bearing mice compared with *6Y OTI* $CD8^+$ T cells in C57BL/6 hosts (Fig. 8c and Extended Data Fig. 8b) and in $Rag1^{-/-}$ hosts (Fig. 8c and Extended Data Fig. 8c), demonstrating that the enhanced in vivo activity of *6F OTI* $CD8^+$ T cells is cell-autonomous.

Retroviral transduction of *6F-CD3ζ* into *OTI* ($CD3ζ^{+/+}$) $CD8^+$ T cells resulted in enhanced in vitro and in vivo tumoricidal activity against B16-F10-V4 melanomas (Fig. 8d,e and Extended Data Fig. 9a–c). Also, *OTI-6F/+* (*6F* heterozygous) $CD8^+$ T cells exhibited enhanced TCR signaling responses to low-affinity ligands (Extended Data Fig. 10a,b), indicating that suppression of endogenous CD3ζ or overexpression of 6F-CD3ζ relative to 6Y-CD3ζ is not required for the 6F-CD3ζ-mediated increase in cytotoxicity or TCR signal enhancement. Finally, transduction of mutated CD3ζ chains where the ITAM tyrosines were substituted with alanine (*6A-CD3ζ*) or deleted (truncated *CD3ζ*) were also capable of enhancing TCR-mediated tumoricidal activity, indicating that this effect is elicited by mutation or removal of CD3ζ ITAMs and is not specific to 6F-CD3ζ (Extended Data Fig. 10c). Collectively, these results suggest that approaches that limit CD3ζ ITAM-mediated negative feedback on TCR signaling represent attractive new avenues for increasing the efficacy of TCR-based cancer immunotherapies.

Discussion

The structural complexity of the TCR, unique among immune receptors in consisting of six signal transducing subunits and ten ITAM signaling motifs, has prompted intensive investigation for three decades with particular interest in determining if the configuration of the TCR can explain its exquisite ligand sensitivity and discrimination. Despite extensive experimentation, a clear mechanistic understanding of how the TCR achieves such impressive sensitivity and discrimination has been elusive, as has evidence supporting specific signaling roles for individual ITAMs or a critical role for ITAM multiplicity in the TCR signaling response, contributing to the perception of the TCR as a fascinating yet enigmatic signaling complex. By employing a 'CD3ζ switch' knock-in experimental mouse model and physiologically relevant readouts of TCR signaling, we discovered an inhibitory function for CD3ζ ITAMs in response to low-affinity ligands that was not detected in previous studies[14,16,36]. Using this model, we ruled out the possibility that the phenotype of *6F(i)* T cells is due to compensatory changes in the expression of signaling molecules or the TCR repertoire imposed during the process of thymocyte selection that occur in germline *6F* mice[14,15].

Our results reveal that CD3ζ performs a dual function in TCR signaling, having a positive (amplifying) or negative (inhibitory) role depending on the affinity of the TCR for its peptide ligand. We also found that the inhibitory function of CD3ζ ITAMs serves as a mechanism for ligand discrimination in response to subthreshold low-affinity peptides as predicted by a new model of adaptive KPR with negative feedback. In contrast to WT 6Y-CD3ζ TCRs, signaling by 6F-CD3ζ TCRs was associated with a dramatic increase in CD3ε, CD3γ and CD3δ ITAM phosphorylation, and, notably, a failure to recruit or retain the inhibitory tyrosine phosphatase SHP1 after TCR engagement. These findings indicate that CD3ζ ITAMs serve primarily to facilitate ligand discrimination by suppressing TCR signaling in response to low-affinity ligands through recruitment of SHP1, contributing only modestly to signal amplification and only in response to high-affinity ligands. They also suggest that the ZAP-70 associated with WT 6Y-CD3ζ ITAMs in resting T cells consists of enzyme in an inhibited rather than an inactive-primed state as speculated previously[53]. Together, our results call for a revision of current models of TCR signaling, which assume that TCR ITAMs have only positive roles in the signaling response[8,9,11,12].

We identified a direct correlation between CD3ζ ITAM phosphorylation and inhibition of TCR signaling in response to low-affinity ligands manifesting as an increased signaling response of 6F-CD3ζ TCRs for all monitored signaling pathways. An inhibitory role for mono-phosphorylated ITAMs has been well established for several other activating immune receptors, including the B cell antigen receptor, the Fcα, Fcγ and Fcε receptors, and Trem2 (ref. 54). In each case, experimental data support the idea that mono-phosphorylation of ITAMs within the signaling subunits of these receptors is responsible for inhibitory ITAM activity through recruitment of the inhibitory phosphatases SHP1 (PTPN6) or SHIP (INPP5D). An inhibitory function for partially phosphorylated CD3ζ ITAMs was previously suggested by results obtained in cell lines with CD8-CD3ζ ITAM mutant chimeras; however, inhibitory ITAM signaling was not demonstrated in the context of the TCR or associated with SHP1 recruitment[17]. Although other explanations are possible, our results

are most consistent with an inhibitory ITAM model where the three tandem CD3ζ ITAMs serve as sites for mono-phosphorylation in response to low-affinity (short dwell time) TCR and peptide–MHC interactions resulting in recruitment (directly or indirectly) of SHP1, thereby attenuating the TCR signaling response. We speculate that the CD3γ, CD3δ and CD3ε ITAMs are more efficiently di-phosphorylated in 6F-CD3ζ TCRs either as result of kinetics (the presence of fewer target ITAM tyrosines for phosphorylation resulting in a higher probability of ITAM di-phosphorylation from short dwell time TCR and peptide–MHC interactions) or possibly due to increased stability of di-phosphorylated or instability of mono-phosphorylated forms of these ITAMs relative to CD3ζ ITAMs, leading to selective recruitment of ZAP-70 over SHP1. Supporting this model are data demonstrating that deletion of *Ptpn6*, the gene encoding SHP1, results in improved TCR signaling responses in $CD8^+$ T cells and increased activity against solid tumors, especially in response to low-affinity ligands[55,56]. Whether the constitutive association of ZAP-70 with WT 6Y-CD3ζ influences the kinetics or ordering of phosphorylation (mono or di) of CD3ζ ITAMs or the recruitment of SHP1 remains to be determined.

Several mechanisms have been proposed for TCR ligand discrimination including TCR and peptide–MHC mechanosensing, selective triggering of inhibitory signaling pathways depending on ligand affinity and kinetic regulation of signaling events downstream of the TCR[3,57,58]. Our results indicate that ligand discrimination is a complex nonlinear process established at the most proximal stage of the TCR signaling response that relies on a balance between positive and negative feedback differentially activated by phosphorylated CD3ζ ITAMs in a ligand-dependent manner. Qualitatively distinct behaviors of *6Y* and *6F* T cells in cytokine LS also suggest that loss of CD3ζ-mediated inhibition explains the reduced discriminatory power of 6F(i) TCRs. Several key predictions of our new mathematical model of KPR with negative feedback, including the loss of ligand discrimination and the transmission of activating signals in response to antagonist ligands by 6F-TCRs, were experimentally validated.

TCR antagonism has remained a long-standing area of interest dating back to the discovery that natural pathogen-encoded APLs are capable of inhibiting T cell activation as a means of immune evasion[59,60]. Recent theoretical work established a consubstantial relationship between sharp ligand discrimination, the need for proximal negative feedback and the existence of antagonism for mixtures of ligands[49]. Although a potential role for CD3ζ ITAMs in TCR antagonism was suggested by early work that identified distinct ITAM phosphorylation patterns in response to agonist and antagonist ligands[19,21–24], a direct causal relationship between CD3ζ ITAM phosphorylation and antagonism was not established. It is unclear if the loss of feedback inhibition and antagonism by 6F-TCRs reflects loss of a CD3ζ-specific regulatory activity or a more general effect caused by reduction in the number of functional TCR ITAMs. Accordingly, it will be of particular interest to determine if the effects of inactivation of CD3γ, CD3δ and/or CD3ε ITAMs on TCR signaling, and in particular on ligand discrimination and antagonism, are similar to or different from those observed after inactivation of the CD3ζ ITAMs.

A limiting factor for current TCR-based adoptive cell therapy approaches for solid tumors, including tumor-infiltrating lymphocytes (TILs), is the relatively low affinity (antigenic

potency) of most tumor-associated antigens[51,52,61]. We showed that T cells expressing TCRs that contain 6F-CD3ζ exhibit an enhanced capacity for controlling the growth of solid tumors expressing poorly immunogenic antigens in mice and can extend the survival of tumor-bearing hosts. Notably, this effect was achieved without increasing TCR ligand affinity, which is frequently associated with 'off-target' autoimmunity[62]. A potential advantage of the 6F-CD3ζ TCR modification is that TILs expressing low-affinity tumor antigen-specific TCRs that otherwise might not actively participate in the antitumor response may be converted to active cytolytic T cells. Thus, our results identify a new approach to adoptive T cell therapies for cancer treatment that may enhance the activity of T cells expressing low-affinity tumor antigen-specific TCRs and also expand the affinity range of effective TCRs.

Methods

Mice

The *6Y*-CD3ζ knock-in *6Y-6F* 'switch' mice were generated as described previously[14]. Distal Lck proximal promoter-driven Cre recombinase (*dLck-Cre*)[34], *Ert2-Cre*[33] or *OX40-Cre*[35] *CD3ζ-6Y/6Y* (*6Y*) mice were crossed to mice transgenic for the *OTI* TCR transgene (The Jackson Laboratory). *CD45.1* and *Thy1.1* congenic mice were obtained from Taconic Biosciences. Genotyping was performed by PCR. Mice were housed in specific pathogen-free conditions at the Eunice Kennedy Shriver National Institute of Child Health and Human Development (NICHD). All animal experiments were performed according to animal care and use committee protocols (ASP no. 15-020; P.E.L.) and approved by the animal care and use committee of the NICHD.

Flow cytometry

Single-cell suspensions were stained with combinations of anti-CD4, anti-CD8, anti-TCRβ, anti-CD69, anti-CD44, anti-CD62L, anti-Thy1.1, anti-Thy1.2, anti-CD45.1, anti-CD45.2, anti-CD25, anti-TCR Vβ5 and anti-TCR Vα2, (BD Biosciences) in PBS (Gibco) with 5% BSA (Sigma-Aldrich). All antibodies were used at a 1:500 dilution. Cells were counted using a Coulter Counter (Beckman Coulter). For intracellular staining, samples were fixed with a BD Biosciences Foxp3 staining kit for intracellular staining according to the manufacturer's directions. Intracellular staining was performed in Foxp3 permeabilization buffer after blocking with 10% normal mouse serum by volume in permeabilization buffer, using an anti-FLAG epitope tag (Sigma-Aldrich), an anti-Myc epitope tag (Cell Signaling Technology), anti-IRF4 (BD Biosciences) or anti-IFNγ (BioLegend). Data were acquired on a BD Biosciences LSR II Flow Cytometer or BD Biosciences LSRFortessa X-20 flow cytometer and analyzed with FlowJo (FlowJo LLC).

In vitro 4-OHT treatment

The *6Y/6Y Ert2-Cre* T cells were cultured in vitro in complete medium complemented with 100 nM of 4-OHT and 100 ng ml^{-1} interleukin-7 (IL-7) for 2 days. Medium was then changed to complete medium with 100 ng ml^{-1} IL-7 and changed every other day for 6 additional days. CD3ζ-6Y or CD3ζ-6F expression was assessed by FLAG and Myc intracellular staining as described in the 'Flow cytometry' section. All control cell

populations (for example, *Ert2-Cre*, *6Y*/*6Y Ert2-Cre*- and *6F*/*6F* T cells) were treated identically with 4-OHT.

In vivo tamoxifen treatment

Mice were orally gavaged daily with 200 μl of a 10 mg ml^{-1} tamoxifen suspension in corn oil for 5 consecutive days. Complete *6Y* to *6F* switch was usually achieved 3 days after the last gavage as assessed by intracellular staining, as described in the 'Flow cytometry' section.

Phosphoflow analysis

Naive *OTI* CD8 T cells were cocultured with irradiated (4,000 rad) APC pulsed with 10^{-5} M of the indicated peptides for 2 min. The reaction was stopped with 10× volume of BD Fix/Perm Transcription Factor Kit phosphoflow buffer and cells were permeabilized using the BD Phosflow Kit and Perm buffer II (BD Biosciences). Cells were stained with PerCP-Cy 5.5 mouse anti-ERK1/2 (pT202/pY204, catalog no. 560115, BD Biosciences), Alexa Fluor 647 mouse anti-LAT (pY171, catalog no. 558518, BD Biosciences) and Alexa Fluor 488 mouse anti-ZAP70 (Y319, catalog no. 557818, BD Biosciences); all were used at a 1:500 dilution. Data were acquired on an LSRFortessa Flow Cytometer (BD Biosciences) and analyzed with FlowJo.

Mixed bone marrow chimeras

Hematopoietic stem and progenitor cells (HSPCs) were enriched from single-cell suspensions of bone marrow by magnetic-activated cell sorting (Miltenyi Biotec) depletion of lineage-positive cells using a cocktail of biotinylated anti-TCRβ, anti-TCRγδ, anti-Ter119, anti-CD3, anti-CD4, anti-CD8, anti-NK1.1, anti-DX5, anti-CD11c and anti-CD11d in combination with streptavidin microbeads (Miltenyi Biotec). $CD45.1^+$ HSPC were mixed 1:1 with $CD45.2^+$ *6Y/6Y Ert2-Cre* HSPCs. Lethally irradiated (950 rad) $CD45.1^+$ hosts were injected retro-orbitally with $2x10^6$ HSPCs. Twelve weeks after injection, mice were treated orally with 2 mg of tamoxifen suspended in corn oil, daily, for 5 consecutive days. Mice were euthanized 2 weeks after the last gavage and T cells were analyzed using FACS.

Cell purification, in vitro activation and CTV labeling

Purified T cell populations were obtained from lymph nodes using a magnetic bead/column system (MACS, Miltenyi Biotec). Naive CD8 T cells were isolated by first labeling total lymph node cells with biotin conjugated anti-B220, anti-CD11b, anti-CD4, anti-Ter119, anti-CD44 and anti-CD25. CD8 T cells (unlabeled fraction) were isolated by magnetic columns after being washed and labeled with streptavidin microbeads. Purity was generally greater than 90%. Cells were activated with the indicated amount of plate-bound anti-CD3 (clone 145-2C11, Bio X Cell), alone or in combination with 1 μg ml^{-1} anti-CD28 (clone 37.51; Bio X Cell) and stained for CD5 or CD69 as described in the 'Flow cytometry' section. For CTV (Molecular Probes) labeling, cells were incubated with 5 mg ml^{-1} of CTV for 15 min at 37 °C then washed three times with complete medium. Cell division was assessed by determining the percentage of $CTV^{lo/med}$ cells by flow cytometry.

Purified APCs were obtained from mouse spleens using a magnetic bead/column system (magnetic-activated cell sorting (MACS); Miltenyi Biotec). Splenocytes were labeled with biotin conjugated anti-CD4, anti-CD8, anti-TCRβ, anti-TCRγδ and Ter119, and then isolated by magnetic columns after being washed and labeled with streptavidin microbeads.

Cell stimulation, calcium assay and immunoblotting

Cell stimulation, calcium mobilization and immunoblotting experiments were performed as described elsewhere[14]. Briefly, $CD8^+$ T cells ($5x10^6$) were stimulated at 37 °C for the indicated times with preformed immune complexes consisting of biotinylated anti-CD3ε (10 μg ml^{-1}; 145-2C11, BD Biosciences) and streptavidin (30 μg ml^{-1}; Sigma-Aldrich) or with the indicated peptide-loaded tetramers (National Institutes of Health (NIH) Emory Tetramer Core Facility) at 300 nM for N4 or 900 nM for Q4/T4/G4. After stimulation, cells were immediately resuspended in lysis buffer containing 0.5% Triton X-100, 10 mM Tris, pH 7.4, 150 mM NaCl, 2 mM Na_3VO_4, 10 mM NaF, 1 mM EDTA and one protease inhibitor tablet (Roche), and were subjected to immunoprecipitation (IP) when applicable. Samples were loaded on 4–12% gradient gels (Invitrogen) and were subsequently analyzed by immunoblot. Antibodies used for blotting or IP included pErk (T202/Y204, catalog no. 9101), pAkt (S473, catalog no. 9271), pZAP-70 (Y319, catalog no. no. 2701; Y493, catalog no. no. 2704), pPLCγ1 (S1248, catalog no. 4510) from Cell Signaling Technologies; pLAT (Y226, catalog no. 558363; Y171, catalog no. 558392) from BD Biosciences; pCD3ζ (Y153, catalog no. MAS-28536) from Invitrogen; ZAP70 (catalog no. sc-32760), CD3ε (catalog no. sc-18871), CD3ζ (catalog no. sc-1239), CD3γ/δ (catalog no. sc-101413) and β-actin (catalog no. sc-69879) from Santa Cruz Biotechnologies; 2A (catalog no. NBP2-59627) from Novus Biologicals; and 4G10 (pan-Tyrosine, catalog no. 05-321) from Merck Millipore. Phospho-specific and total protein antibodies were used at 1:500 and 1:1000 dilution, respectively. Immunoblots were analyzed with the Azur cSeries capture software. For the calcium assay, cells were loaded with Indo-1 (Invitrogen) and stimulated with the indicated peptide-loaded tetramers (NIH Emory Tetramer Core Facility) at 15 nM for N4 or 60 nM for Q4/T4/G4, followed by ionomycin after 6 min.

Cytokine induction

Naive *OTI* CD8 T cells were cocultured with irradiated (4,000 rad) APCs pulsed with the indicated concentration of peptides for 1–3 days depending on the experiment and then stained with the indicated antibodies as described in the ‘Flow cytometry’ section. For the antagonism assays, APCs were pulsed with the indicated concentration of agonist peptide (for example, N4 or Q4) for 1 h, washed three times with PBS, then pulsed with the indicated amount of antagonist peptide (for example, V4, G4 or E1) for 1 h and washed three times before the coculture assay. Cytokine measurement was performed on 3-day culture supernatants as described in the ‘CBA measurement’ section.

In vivo proliferation assay

Purified *Thy1.1* WT and *Thy1.2 6Y/6Y Ert2-Cre* cells were cultured in vitro with 4-OHT, stained with CTV as described above and then mixed 1:1; $2x10^6$ cells in 100 μl PBS were injected retro-orbitally into *Thy1.1/Thy1.2* mice and $3x10^6$ irradiated (4,000 rad) APCs pulsed with 1 mM of the indicated peptide were injected the following day. Mice were

euthanized 6 days later and cell proliferation was assessed by CTV dilution in spleen and lymph node T cells by flow cytometry.

Virus infections and immunizations

Eight to 12-week-old sex-matched *6Y/6Y, 6Y/6Y OX40-Cre* and *6F/6F* mice were infected intravenously with $2x10^6$ plaque-forming units of LCMV Armstrong clone 53b. Stocks were prepared by a single passage on BHK-21 cells; viral titers were determined by plaque formation on Vero cells.

For the stimulation of T cells after LCMV infection, the following peptides were used: GP61-80, NP396-404, GP33-41, NP205-212 and GP276-286 (GenScript).

Robotics

T cell cultures were prepared as follows. C57BL/6N (B6) splenocytes were pulsed with peptide for 2 h at 37 °C, washed once and used as APCs. Fifty thousand *OTI* CD8 T cells were mixed with 300,000 antigen-pulsed APCs in 200 µl complete Roswell Park Memorial Institute 1640 medium (final volume), in 96-well V bottom plates and were then spun at 500*g* for 10 s to form contacts. Plates were immediately loaded into a Tecan robotic platform to start the timed acquisition. The robotic platform was programmed to perform automatic collection and replenishment of supernatant at given time points (typically 1, 3, 6, 12, 18, 24, 30, 36, 42, 48, 60 and 72 h after initiation). At each time point, the robot retrieved the cell coculture plates and aspirated 10 µl of culture supernatant from the coculture plates, transferred this collected supernatant to a separate collection plate (cooled to −2 °C to prevent evaporation) and finally replenished the culture plates with 10 µl of fresh medium to keep the total volume of medium in the culture plate the same throughout the experiment. Collected supernatants were stored at −20 °C until CBA measurement.

CBA measurement

We used a mouse Th1/Th2/Th17 CBA kit from BD Biosciences to quantify seven cytokines in each collected supernatant. Collected supernatants were thawed at room temperature, loaded with CBA reagents (beads and detection reagents) and incubated at room temperature for 15 min. To multiplex acquisition using flow cytometry, plates were then barcoded using fluorescently labeled Fab fragments. Typically, Dy405-labeled or FITC-labeled anti-Rat Fab fragment (Jackson ImmunoResearch) were added to a final concentration of 2 µg ml^{-1} and incubated for 15 min at room temperature. This reaction was then quenched by adding an excess of rat IgG (Jackson ImmunoResearch) to a final concentration of 30 µg ml^{-1} and incubated for 15 min at room temperature. Fab-labeled CBA plates were then consolidated into one plate, spun down at 1,000*g* for 2 min, flipped to discard supernatant, gently vortexed and finally resuspended in 100 µl of FACS buffer (4% FCS (Atlas Biologicals) + 1 mM sodium azide (Sigma-Aldrich) in PBS (Lonza)) for acquisition on a 5-laser, 18-channel flow cytometer (LSRFortessa, BD Biosciences).

Data analysis

CBA flow cytometry standard files were exported and then converted to labeled Excel files for statistical analysis using the high-throughput data processing pipeline plateypus (https://

github.com/soorajachar/plateypus). The tutorial PowerPoint linked on this page contains detailed instructions on use.

Tumor cell lines

B16-F10-mKate2-OVA/A2/Y3/Q4/T4/V4 cell lines were generated by J. Davies by transducing a new aliquot of B16-F10 cells (catalog no. CRL-6475, ATCC) transduced with retroviral vectors. All cell lines were cultured in complete medium containing DMEM (Gibco), 10% FCS (GE Healthcare), 10 mM HEPES (Gibco), 2 mM GlutaMAX (Gibco), 100 IU ml^{-1} penicillin and 100 μg ml^{-1} streptomycin (Gibco), 1× non-essential amino acids (Gibco) and 50 μg ml^{-1} gentamicin (Gibco). All cell lines were grown in a humidified incubator with 5% CO_2 at 37 °C and were routinely tested for *Mycoplasma* contamination.

Mouse $CD8^+$ T cell isolation, activation and expansion

For experiments where T cells were not retrovirally transduced, *OTI* splenocytes were stimulated with 0.5 μM SIINFEKL peptide (GenScript) and plated at 3×10^6 per ml in 24-well plates. The next day, 1 ml of complete medium supplemented with 60 IU ml^{-1} IL-2 (aldesleukin, Prometheus) was added to each well. Cells were split as needed and fed daily with complete medium containing 60 IU ml^{-1} IL-2 from this point forward.

For experiments where T cells were to be retrovirally transduced, *OTI* splenocytes were plated at the same density as above into 24-well plates coated with plate-bound anti-CD3ε (clone 145-2C11, Bio X Cell) at 2 μg ml^{-1} and supplemented with soluble anti-CD28 (clone 37.51 from Bio X Cell) at 1 μg ml^{-1}. As with peptide stimulation, 1 ml of complete medium containing 60 IU ml^{-1} IL-2 was added to each well the day after the initial stimulation. On day 2, all cells were collected, washed and plated in complete medium containing 60 IU ml^{-1} IL-2 at $5x10^5$ to $1x10^6$ cells per ml into 24-well plates coated with retronectin (Takara Bio) at 20 μg ml^{-1} and absorbed with the respective retroviral vector. The following day, cells were fed with 1 ml of complete medium containing 60 IU ml IL-2. On day 4 after stimulation, cells were removed from the retronectin-coated plate and seeded at 1×10^6 cells per ml into 24-well plates and split as needed. In all experiments both in vitro and in vivo, the resulting T cells were used on day 6 after the initial stimulation.

In vivo tumor inoculation, adoptive T cell transfer and treatment

For the in vivo tumor treatment experiments, tumor cell lines were injected subcutaneously at 1×10^6 cells in 50 μl of Hanks' Balanced Salt Solution (HBSS) into the right flank of 6–10-week-old C57BL/6J or B6.*Rag1* knockout mice on day −7. On day −1, mice were subjected to single-dose total body irradiation at 5.5 Gy; their tumor was measured with calipers by first measuring the longest edge of the tumor followed by measuring at a 90° angle to the first measurement. Mice without established palpable tumors or mice with tumors resulting from poor injections were not included in the tumor cohorts. The remaining mice were randomized into the groups within the cohort. Adoptive T cell therapy experiments were initiated on day 0 by injecting 1×10^6 to 1×10^7 T cells into tumor-bearing hosts via intraperitoneal injections in 200 μl of HBSS. Tumors were measured twice weekly until the endpoint criteria were met.

Cytotoxic killing assay

The in vitro cytotoxic killing assays were performed using an Agilent xCELLigence RTCA MP instrument to measure label-free cellular impedance. B16-F10 tumor cells were seeded at 10,000 cells per well in a p96 RTCA E-Plate (Agilent Technologies) the day before adding the T cells. Activated effector T cells (T_{eff}) were added on day 6 after in vitro activation, as described above, at the indicated effector-to-target ratios. The xCELLigence instrument was set to measure impedance every 15 min throughout the duration of the experiment. Data were normalized to the time point immediately preceding the addition of T_{eff} cells, according to the manufacturer's recommendation.

Statistical analysis

Statistical analyses were performed as described in the figure legends using Prism (GraphPad Software).

In vivo tumor assay statistical analysis

This work was done using SAS v.9.4 (SAS Institute). The primary characteristic of the data from the tumor models in this investigation was a phenomenon known as informative (dependent) censoring. The fundamental goal of the research was to examine the growth of tumors over time; however, in some instances, animals had to be euthanatized when their tumors grew to such an extent that mice would have experienced stress due to the burden of the induced lesion. Because euthanasia of these animals resulted in incomplete growth curve information, these data are referred to as censored. Typically, censoring is non-informative (non-dependent) when the loss of data could not be attributed to a specific condition within the experiment, for example, the random death of an animal for reasons independent of its treatment group or the size of the tumor (e.g. a spontaneous infection or other cause).

To mitigate these circumstances, we used the methodology described by Vardi et al.[63]. Instead of using the means of individual values of tumor growth at each time point to compare the groups, we used the area under the tumor growth curve as a surrogate. This is not unnatural insofar as a tumor growth curve for a tumor that grows quickly will typically have a greater area under its curve. Briefly, the area under the curve (estimated by the commonly used trapezoidal method) for each animal in one group was compared with the area under the curve for each animal in another group, but only for the portion of the curve that was in common. Thus, if one animal had to be euthanized at a time t, while a second animal lived to a longer time (for example, $t + 3$), the areas under the curves for these two animals would only be compared up to the time t. The differences could then be compared under the null hypothesis of no group effect (essentially, the 'typical' difference was close to zero) via a Wilcoxon signed-rank test. To ensure preservation of the nominal level of statistical significance, these P values were then adjusted using an approach derived from Hommel's procedure.

Extended Data

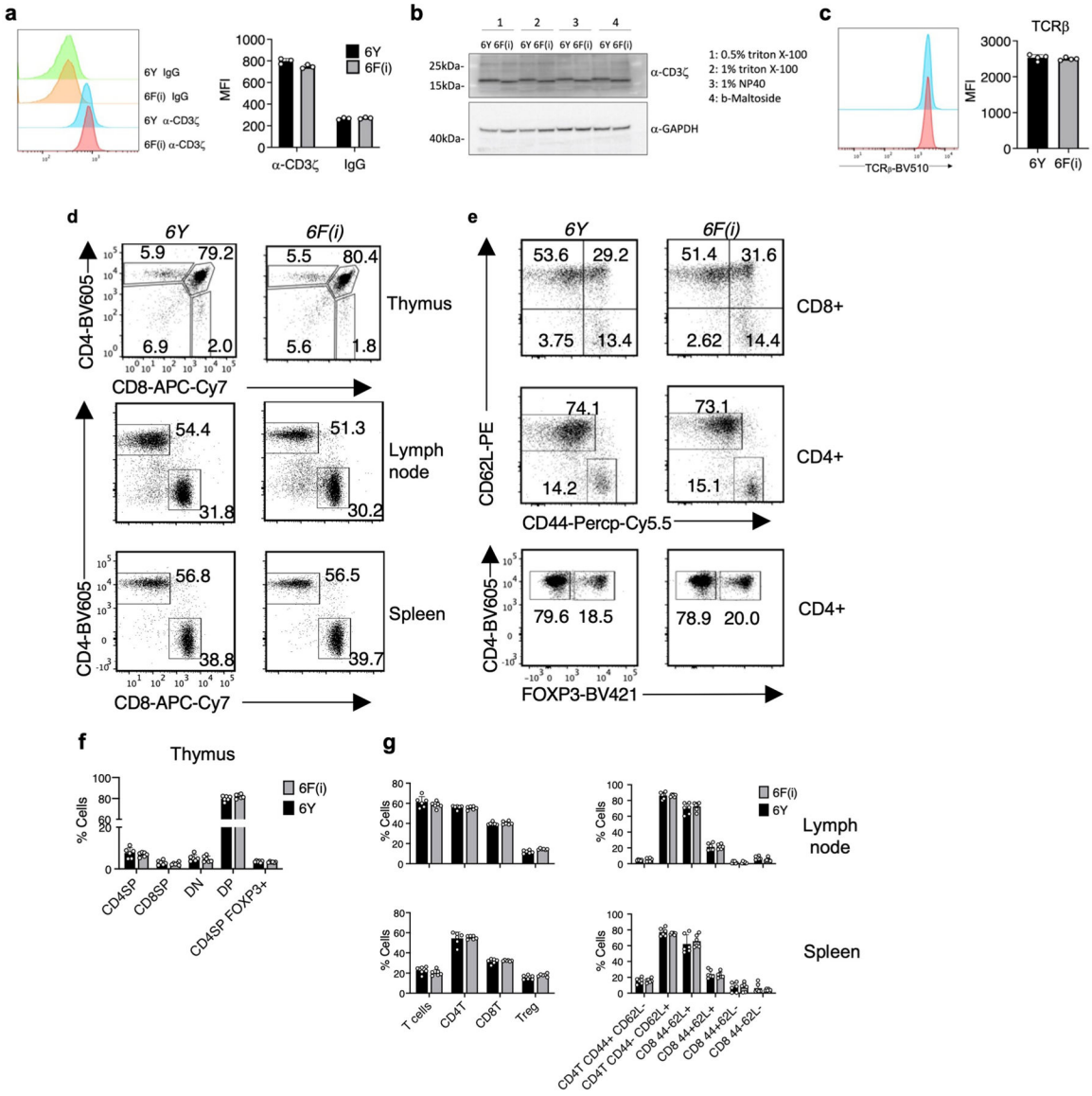

Extended Data Fig. 1 |. 6Y and 6F CD3ζ protein variants are expressed at the same level in peripheral T cells and *6Y* and *6F(i)* mice have similar phenotypes.

CD8$^+$ T Cells from *6Y/6Y dLck-Cre- [6Y]* and *6Y/6Y dLck-Cre + [6F(i)]* mice were analyzed for CD3ζ expression by: **(a)** Intracellular staining with anti-CD3ζ and FACS acquisition (representative plot on left, summary graph on right), or **(b)** Western blot with anti-CD3ζ after cell lysis using the indicated detergents. (**c**) Surface TCRβ levels (MFI) were determined by antibody staining and FACS (representative plot on left, summary graph on right). **d-g,** Phenotype of *6Y/6Y OX40-Cre- [6Y] and 6Y/6Y OX40-Cre + [6F(i)]* mice. (**d**) Flow cytometry analysis of CD4/8 populations in Thymus, Spleen and Lymph nodes. **(e)** Flow cytometry analysis of naïve/memory and Treg populations in Spleen. (**f,g**) Plots showing the percentage of indicated cell populations in the thymus (**f**) and Lymph node/

Spleen (**g**) of *6Y* and *6F(i)* mice. Data are expressed as mean value ± SD). Plots shown are representative of at least three experiments with two mice per genotype.

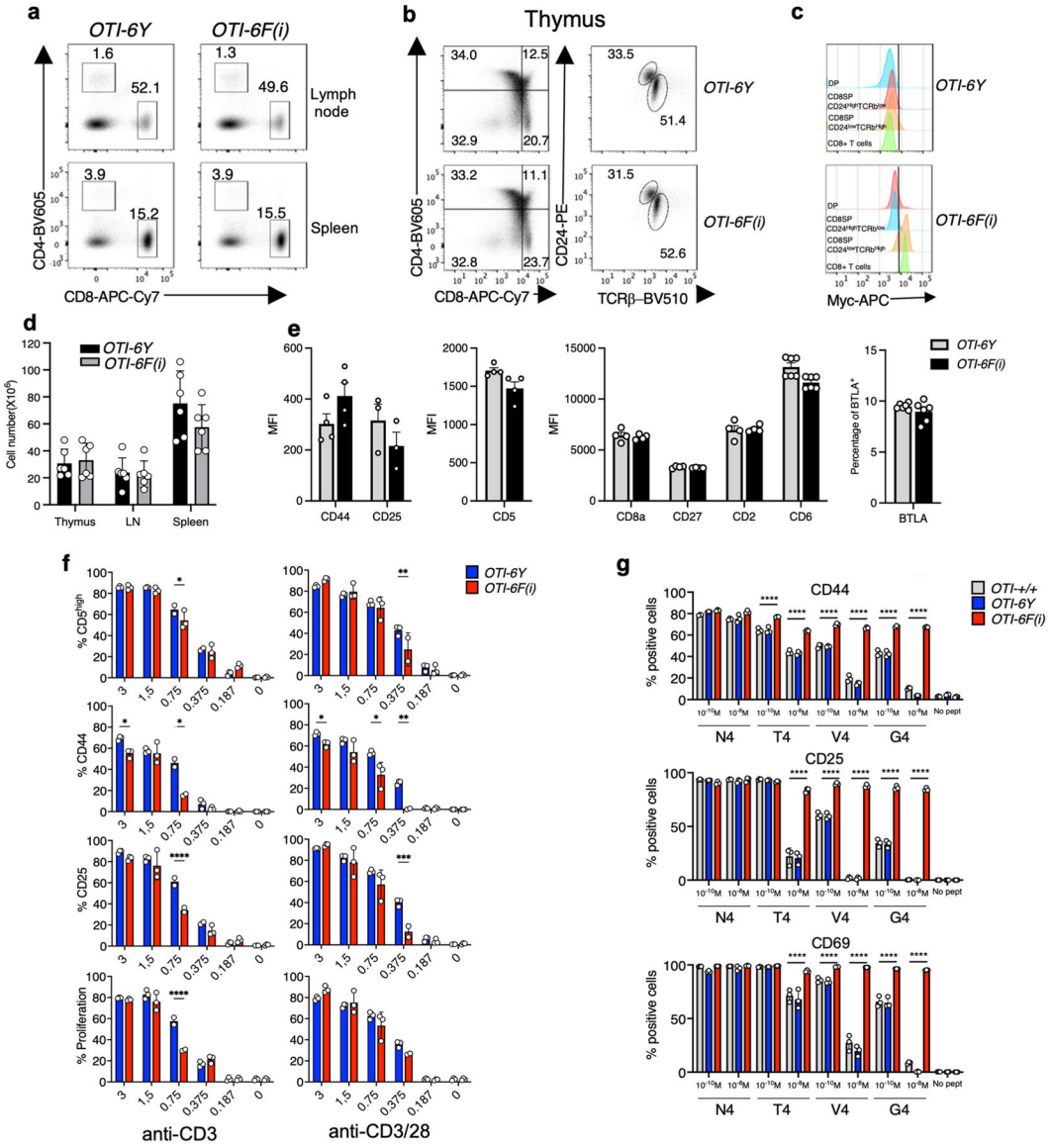

Extended Data Fig. 2 |. Phenotype of *OTI 6Y/6Y dLck-Cre- [OTI-6Y] and* OTI 6Y/6Y dLCK-Cre + [*OTI-6F(i)*] mice.

(**a,b**) Flow cytometry analysis of Spleen and Lymph nodes **(a**) or thymus **(b**). Data are representative of at least three experiments with two mice per genotype. (**c**) Intracellular staining showing expression of CD3ζ-6F-Myc in double positive (CD4+ CD8+ ; DP), immature ($CD24^{High}$ $TCR\beta^{low}$) and mature ($CD24^{Low}$ $TCR\beta^{High}$) CD8 SP thymocytes and peripheral $CD8^+$ T cells from *OTI-6Y* and *OTI-6F(i)* mice. (**d)** Cellularity of thymus, or pooled axillary, brachial and inguinal lymph nodes (LN) and spleen of *OTI-6Y* and *OTI-6F(i)* mice. Data are expressed as mean value ± SD (n = 6 mice from three independent experiments). **(e)** $CD8^+$ T cells from *OTI 6Y/6Y dLck-Cre- [6Y]* and *OTI 6Y/6Y dLck-Cre + [OTI-6F(i)]* mice were analyzed for key threshold TCR signaling regulators by FACS

analysis. Data are expressed as mean value ± SD (n = 4 mice from two independent experiments). **(f)** CD5, CD44, CD25 and CD69 activation marker expression, and CTV dilution (proliferation), by/of peripheral naive *OTI-6Y* and *OTI-6F(i)* CD8+ T cells stimulated with increasing amounts of anti-CD3 (μg/ml) alone (left panel) or in combination with anti-CD28 (1 μg/ml) (right panel). Data are expressed as mean value ± SD (n = 3 biological replicates). Data representative of three independent experiments. **(g)** *OTI* WT [*OTI* + /+], *OTI 6Y/6Y dLck-Cre-* [*OTI-6Y*] and *OTI-6Y/6Y dLck-Cre* + [*OTI-6F(i)*] T cells were co-cultured with APC pulsed with 10^{-8} M or 10^{-10} M of the indicated peptide for 24 h and the expression of the indicated activation markers was analyzed by FACS. Data are expressed as mean value ± SD (n = 3 biological replicates). Data representative of two independent experiments. *P < 0.05, **P < 0.01, ***P < 0.001, ns not significant.

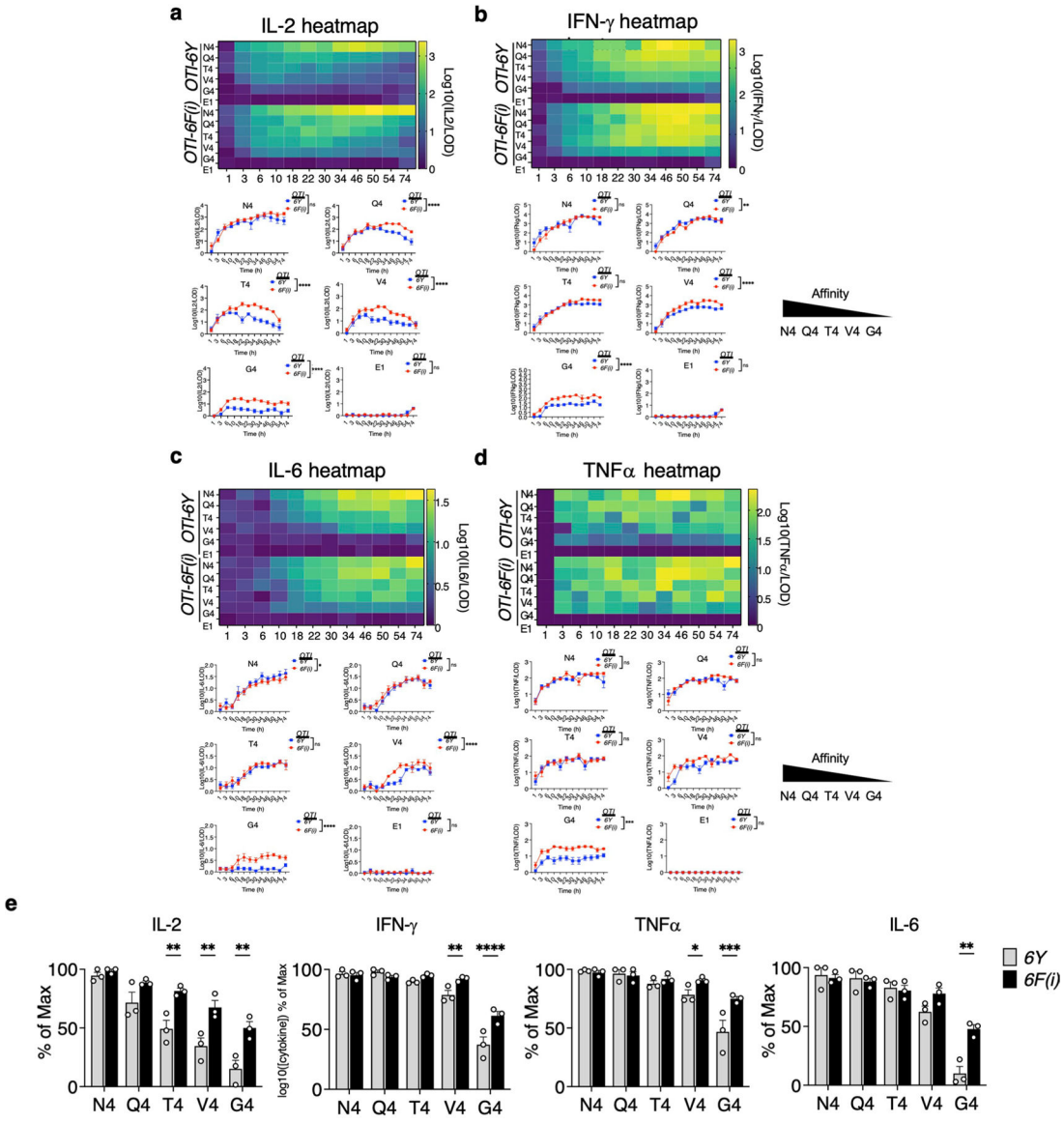

Extended Data Fig. 3 |. 6F-CD3ζ-expressing CD8$^+$ T cells have a lower threshold of activation by low affinity antigens. Related to Fig. 2.

CD8$^+$ T cells from *OTI 6Y/6Y dLck-Cre- [OTI-6Y]* and *OTI 6Y/6Y dLck-Cre + [OTI-6F(i)]* mice were co-cultured with APC pulsed with 10^{-6} M of the indicated peptide and accumulation of: (**a**) IL-2, (**b**) IFNγ, (**c**) IL-6, or (**d**) TNFα was assessed in the culture supernatants at the indicated times. Heatmaps of cytokine expression are shown on top. Bottom, Graphs of cytokine measurements are shown as Log10(cytokine/LOD), where LOD is the limit of detection. Data are represented as mean ± SEM. Statistical significance determined by two-way ANOVA corrected with Sidak test for multiple comparison. Data are representative of 8 independent experiments. **(e)** *OTI 6Y/6Y [OTI-6Y]* and *OTI 6Y/6Y Ert2-Cre + [OTI-6F(i)]* CD8+ T cells were treated *in vitro* with 4-OH tamoxifen for 48 hr before stimulation experiments. T cells were co-cultured with APC pulsed with 10^{-6} M of the indicated peptide and accumulation of IL-2, IFNγ, IL-6 or TNFα was assessed in the culture supernatants. Graphs of cytokine measurements are shown as mean of logarithm of concentrations over the whole time-course of the experiment, normalized by the lower limit of detection (LOD) in supernatant. N = 3 biological replicates from three independent experiments. Data are represented as mean ± SEM. Statistical significance determined by two-way ANOVA corrected with Sidak test for multiple comparison. *$p < 0.05$, **$p < 0.01$, ***$p < 0.001$, ****$p < 0.0001$, ns, not significant.

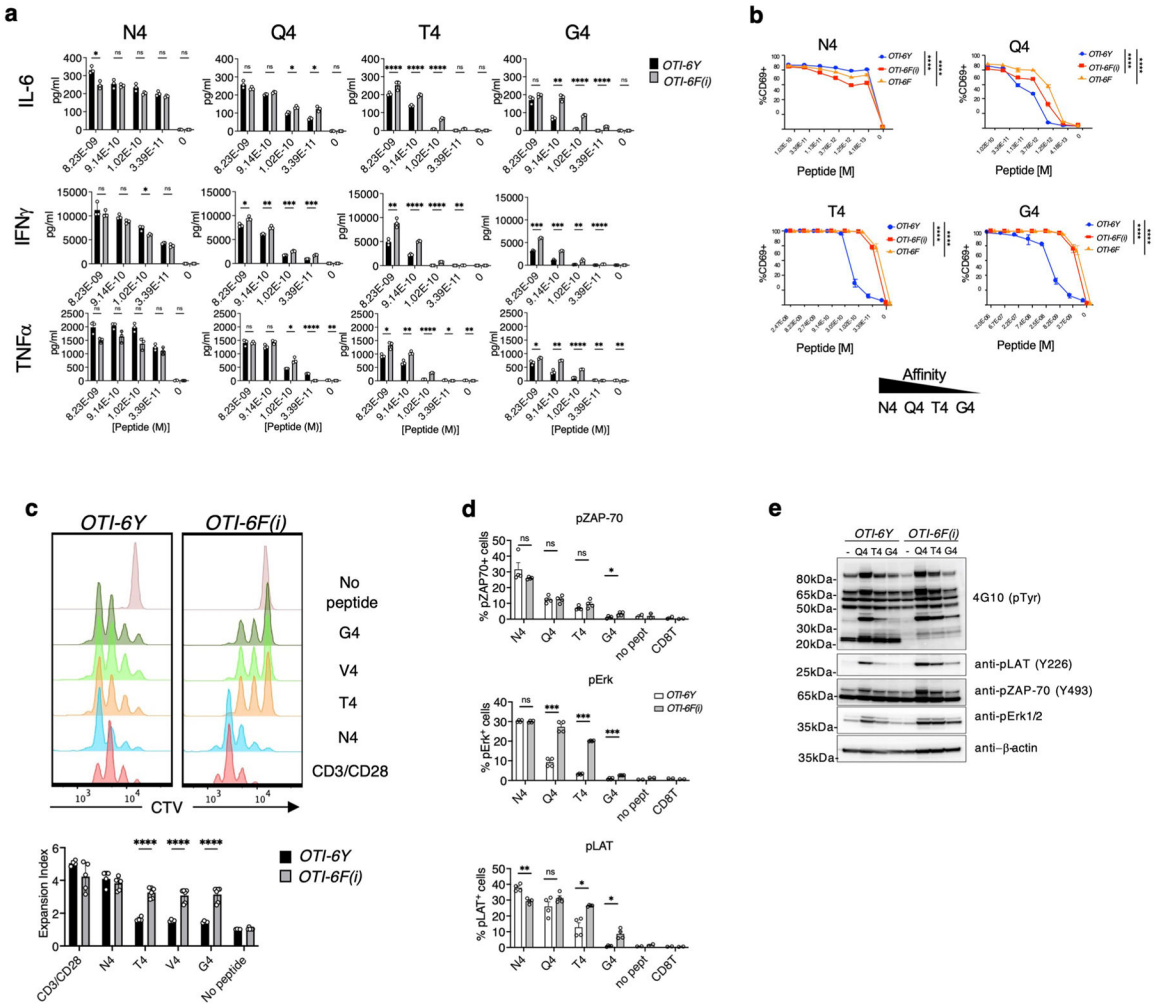

Extended Data Fig. 4 |. The enhancing effect of 6F-CD3ζ on TCR signaling in response to low affinity ligands is diminished when the ligand concentration (avidity) is increased. Related to Fig. 2.

4-OH tamoxifen treated *OTI 6Y/6Y [OTI-6Y]* and *OTI 6Y/6Y Ert2-Cre + [OTI-6F(i)]* $CD8^+$ T cells (**a**) or *OTI 6Y/6Y [OTI-6Y], OTI 6Y/6Y dLck-Cre + [OTI-6F(i)], and* germline *OTI 6F/6F [OTI-6F]* $CD8^+$ T cells (**b**) were stimulated with APC pulsed with the indicated concentration of peptides and analyzed for cytokine production in the supernatant (**a**) or CD69 surface expression by FACS (**b**). Statistical significance determined by unpaired two-sided t-test analysis (**a**) or two-tailed ANOVA test analysis (**b**). Data are represented as Mean ± SEM. N = 3 biological replicates, Data representative of three independent experiments. *$p < 0.05$, **$p < 0.01$, ***$p < 0.001$, ****$p < 0.0001$, ns, not significant. Data are from three independent experiments. **c**, **d**, **e**, 6F-CD3ζ-expressing T cells have a lower threshold of activation toward low affinity antigens. Related to Fig. 3**. (c)** Proliferation of $CD8^+$ T cells from *OTI 6Y/6Y dLck-Cre- [OTI-6Y]* and *OTI 6Y/6Y dLck-Cre + [OTI-6F(i)]* mice co-cultured for 72 h with APC pulsed with 10^{-6} M of the indicated peptide assessed by Cell Trace Violet (CTV) dilution. Summary of experiments are shown in the graph below. N = 5 biological replicates from 2 independent experiments. Data are represented as Mean ± SEM. Statistical significance determined by two-way ANOVA corrected with Sidak test

for multiple comparison. (**d**), *OTI* CD8$^+$ T cells from *OTI 6Y/6Y [OTI-6Y] or* OTI 6Y/6Y *dLck-Cre* + *[OTI-6F(i)]* mice were stimulated for 2 minutes with peptide-pulsed APCs. Graph represents the percentage of pZAP-70 (Y319), pLAT (Y171) or pErk1/2 (T202/Y204) positive cells from intracellular staining. Data were analyzed by unpaired t-test (two tailed) and are represented as mean ± SEM. *P < 0.05, **P < 0.01, ***P < 0.001, ****P < 0.0001. (**e**), *OTI-6Y* and *OTI 6Y/6Y Ert2-Cre* + *[OTI-6F(i)]* CD8$^+$ T cells were treated *in vitro* with 4-OH tamoxifen for 3 days, stimulated for 2 min with the indicated Kb peptide-tetramers, lysed and analyzed by PAGE and immunoblot with the indicated antibodies. Data are representative of three independent experiments.

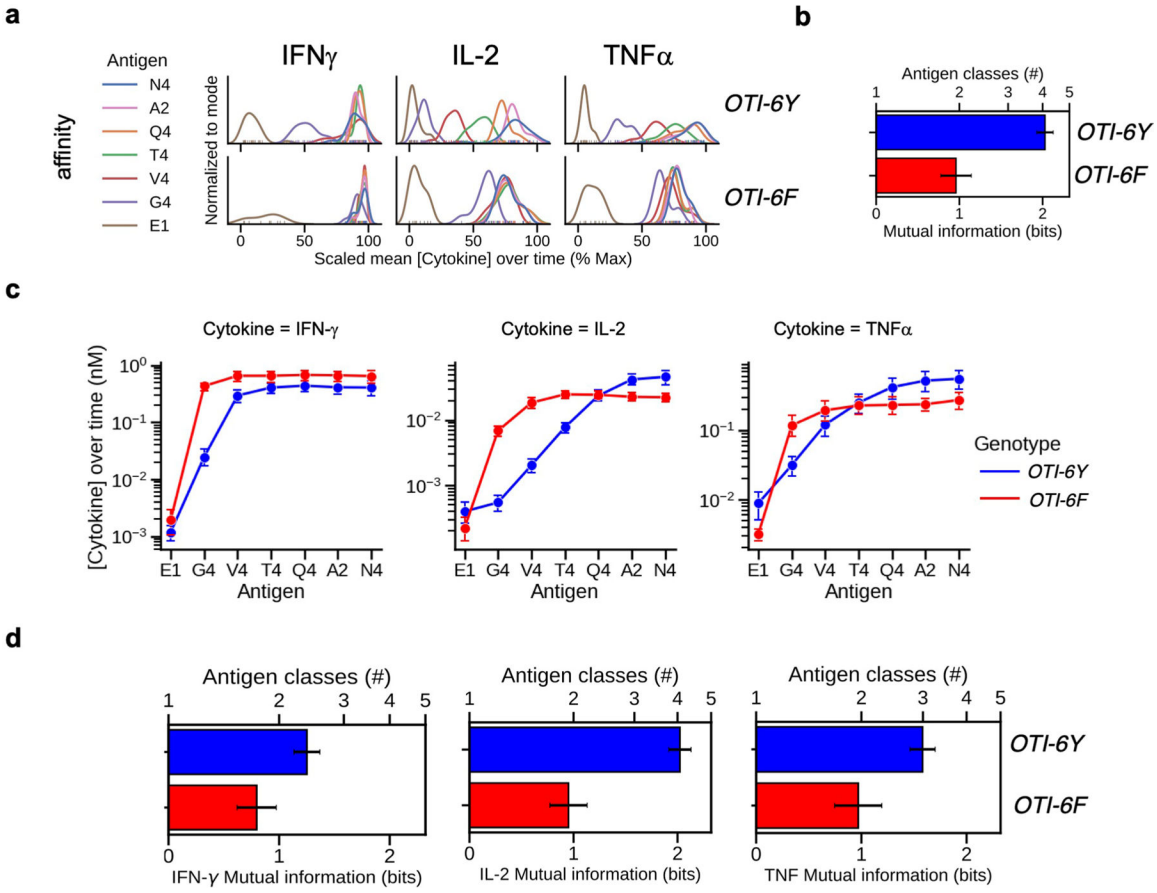

Extended Data Fig. 5 |. Analysis of the cytokine release profile of germline *OTI-6F* CD8$^+$ T cells over a 72 hr time course. Related to Fig. 4.

(a) Distribution of cytokine secretion levels of effector *OTI-6Y* or *OTI-6F* (germline) CD8$^+$ T cells pre-stimulated with 10^{-6} M-*6* N4 antigen + APCs for 6 days then re-stimulated with APC + 10^{-6} M antigens of varying affinities.(**b**) Mutual information (antigen classes) between antigen quality and all secreted cytokines for each genotype. While *OTI-6Y* T cells can distinguish more than four classes of antigen across the 6 peptide affinities tested, *OTI-6F* T cells only distinguish two. Data are expressed as MI estimator ± SD.**(c)** Summary plots of cytokine secretion showing scaled mean over time. Data are represented as mean ± SD. (**d**) Mutual information (antigen classes) between antigen quality and each secreted

cytokine for each genotype. Data are expressed as MI estimator ± SD. **(**[n = 14 *OTI-6Y* (*OTI 6Y/6Y*) or n = 10 *OTI-6F* (*OTI 6F/6F*) biological replicates].

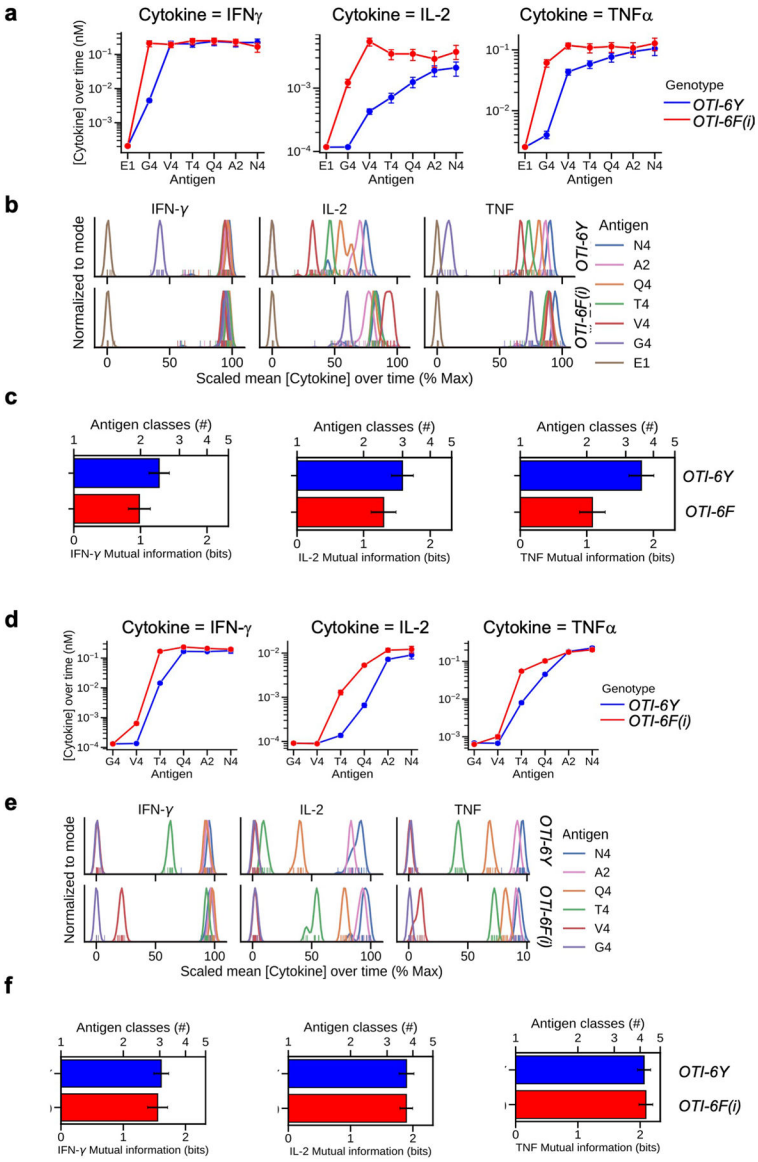

Extended Data Fig. 6 |. Analysis of the cytokine release profiles of *OTI-6F(i)* CD8$^+$ blasts restimulated with 10^{-6} M peptide (a-c) or 10^{-9} M peptide (d-f) over a 72 h time course. Related to Fig. 4.

(a-c), *OTI-6Y* (*OTI 6Y/6Y dLckCre-*) and *OTI-6F(i) (OTI 6Y/6Y dLckCre+*) CD8+ T cells were co-cultured with APC pulsed with 10^{-6} M N4 peptide for 6 days then re-stimulated with APC + 10^{-6} M antigens of varying affinities. **(a)** Distribution of cytokine secretion levels. Data are represented as mean ± SD. **(b)** Summary plots of cytokine secretion showing scaled mean over time. **(c)** Mutual information (antigen classes) between antigen quality and each secreted cytokine for each genotype. N = 3 biological replicates. Data are expressed as MI estimator ± SD.**(d-f)** *OTI-6Y* and *OTI-6F(i)* CD8+ T cells were co-cultured with APC pulsed with 10^{-6} M N4 peptide for 6 days then re-stimulated with APC + 10^{-9} M antigens

of varying affinities. **(d)** Distribution of cytokine secretion levels. Data are represented as mean ± SD. **(e)** Summary plots of cytokine secretion showing scaled mean over time. **(f)** Mutual information (antigen classes) between antigen quality and each secreted cytokine for each genotype. N = 3 biological replicates. Although MI/Antigen class plots are similar for *OTI-6Y* and *OTI-6F(i)* T cells due to the enhanced response of *OTI-6F(i)* T cells to low affinity ligands, *OTI-6F(i)* T cells exhibit reduced discrimination of mid-high affinity ligands. Data are expressed as MI estimator ± SD.

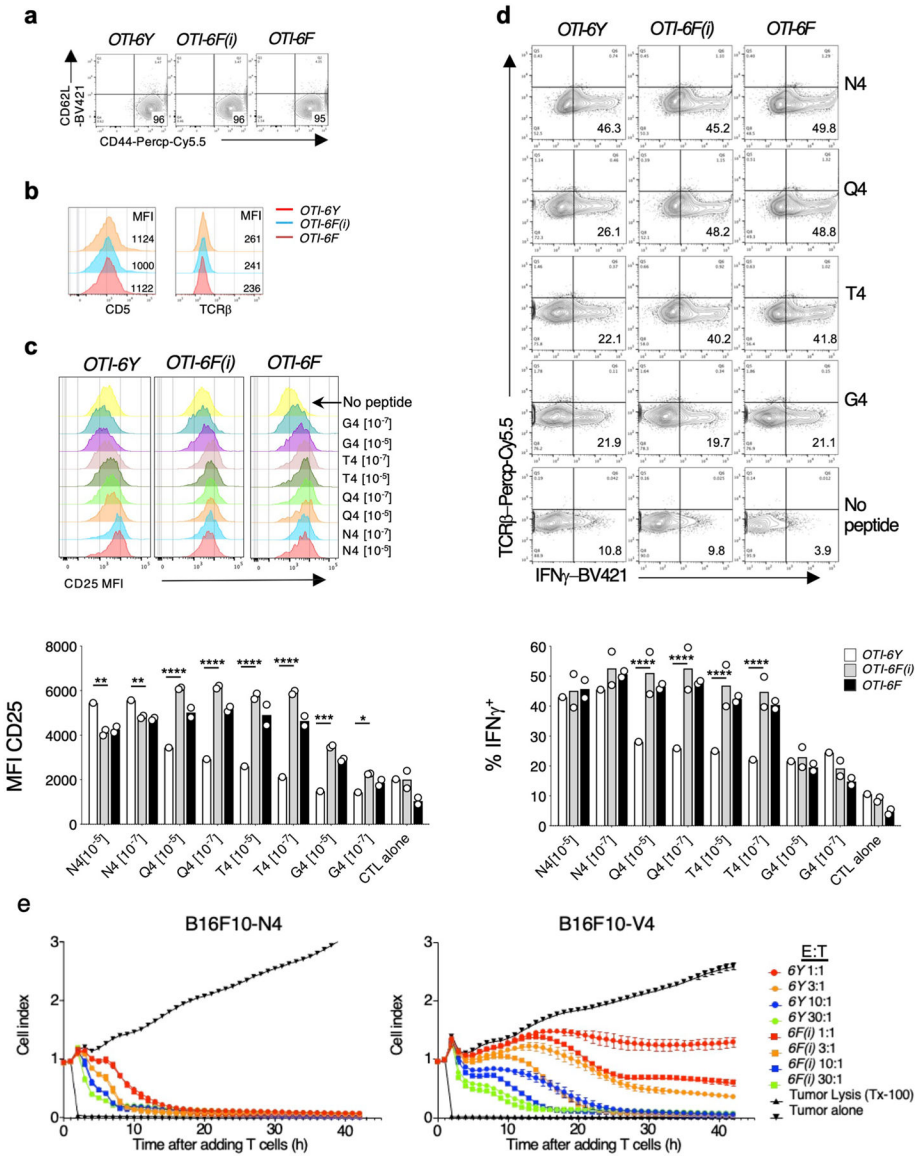

Extended Data Fig. 7 |. Activated and expanded 6F-CD3ζ-expressing CD8$^+$ T cells exhibit a lower threshold of activation toward low affinity peptides. Related to Fig. 8.

OTI-6Y [OTI 6Y/6Y-Ert2-cre-]; OTI-6F(i) [OTI 6Y/6Y Ert2-Cre+]; and OTI-6F germline [*OTI 6F/6F]* T cells were treated *in vitro* with 4-OH tamoxifen for 48 hr then activated *in vitro* with 0.5x10^{-6} M N4 peptide for 6 days before secondary stimulation experiments. (**a**), FACS analysis showing CD62L vs CD44 surface staining, or (**b**), CD5 and TCRβ

surface staining (Mean Fluorescence Intensity; MFI) of *OTI* $CD8^+$ T cells of the indicated genotypes after *in vitro* activation and expansion. (**c,d**) Activated and expanded *OTI* CD8 T cells were re-stimulated with APC pulsed with the indicated peptides and analyzed by FACS for CD25 surface expression **(c)** or IFNγ expression **(d)** by intracellular staining. Bar graph plots show MFI of CD25 (left) or % IFNγ^+ cells (right) from experiments shown in (c) and (d), respectively. Statistical significance determined by unpaired t-test analysis. *p < 0.05, **p < 0.01, ***p < 0.001,****p < 0.0001, ns, not significant. Data are representative of at least two experiments. (**e**) *OTI* $CD8^+$ T cells of the indicated genotypes were treated *in vitro* with 4-OH tamoxifen for 48 h and activated with $0.5x10^{-6}$ M N4 peptide for 6 days before experiments. *OTI-6Y [OTI 6Y/6Y Ert2-cre-]; OTI-6F(i) [OTI 6Y/6Y Ert2-cre+]*. Shown are *in vitro* killing assays of *OTI* $CD8^+$ T cells from the indicated mice against B16 F10-N4 (left) or B16 F10-V4 (right) target cells at the indicated effector-to-target ratios by xCELLigence RTCA (Agilent). Data are represented as mean ± SD.

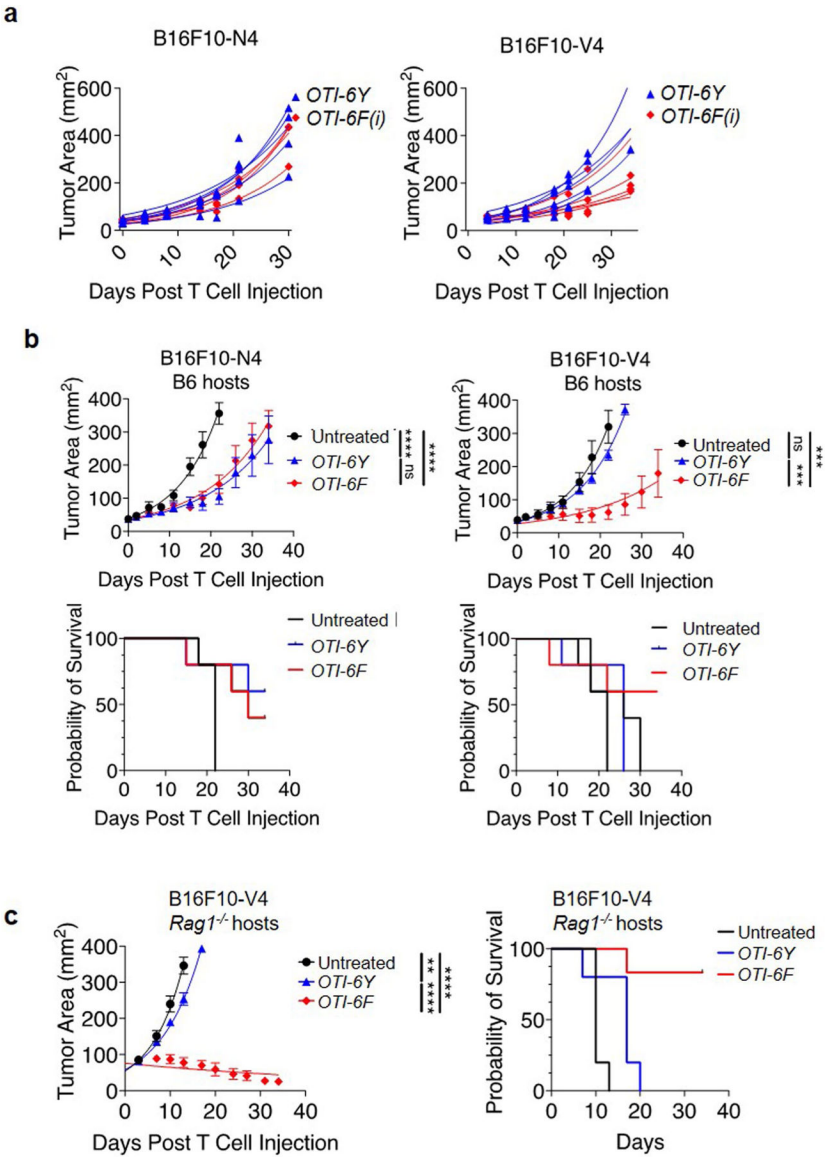

Extended Data Fig. 8 |. 6F-CD3ζ-expressing CD8$^+$ T cells exhibit higher cytotoxicity toward tumor cells expressing low affinity (V4) ligand. Related to Fig. 8.

(a) Plot showing individual tumor measurements related to Fig. 8b. (**b**) C57B6 mice were injected with pre-activated (0.5x10^{-6}M N4 peptide) *OT1-6Y or OTI-6F* CD8$^+$ T cells 7 days after B16F10-V4 melanoma implantation. Results shown are representative of 3 experiments. Top, measurement of the size of B16F10-N4 or B16F10-V4 tumors implanted into C57B6 mice. Bottom, survival curves of experiment shown above. Data are represented as mean ± SD **(c)** Left, *Rag2*$^{-/-}$ mice that were injected with pre-activated (0.5x10-6M N4 peptide) *OT1-6Y or OTI-6F* CD8+ T cells 7 days after B16F10 melanoma implantation. Right, survival curves of experiments shown on left. Results shown are representative of 3 experiments. Data are represented as mean ± SD. *P < 0.05, **P < 0.01, ***P < 0.001, ****P < 0.0001, ns, not significant.

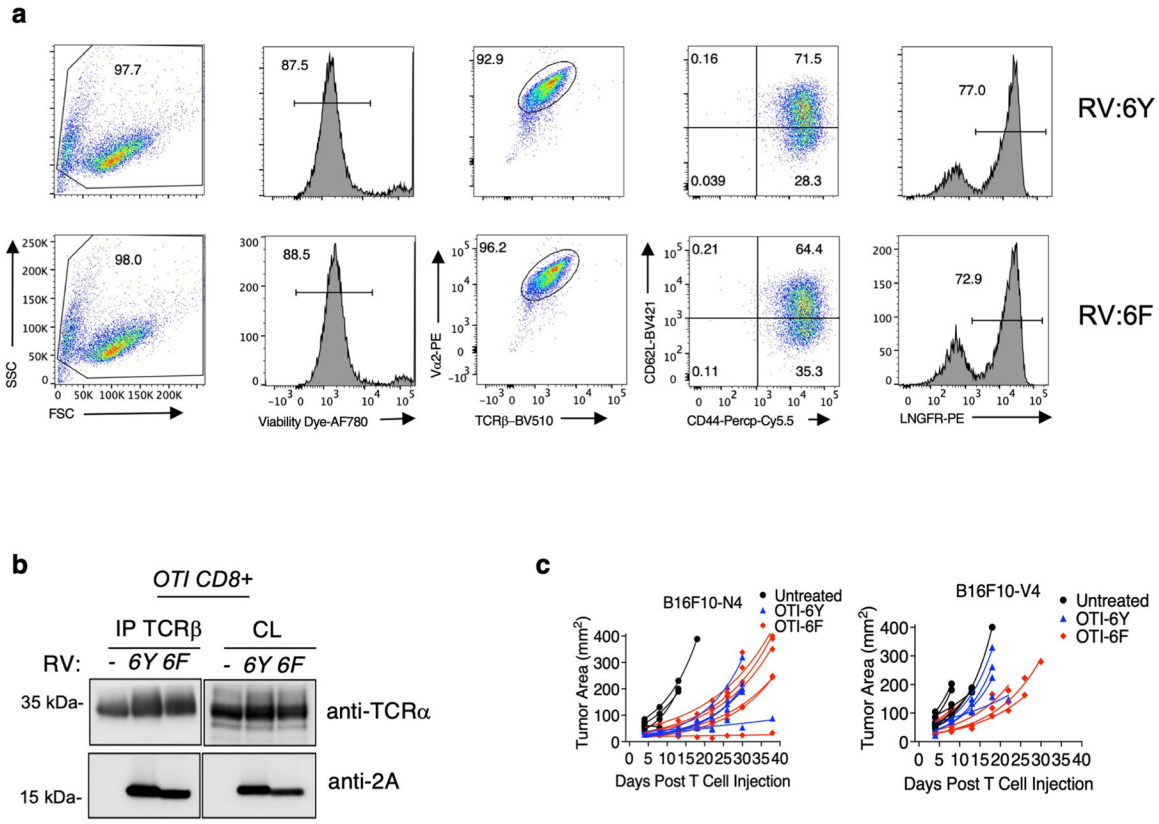

Extended Data Fig. 9 |. Retroviral (RV) transduction of 6F-CD3ζ^{z} into WT (+/+) *OTI* CD8^{+} T cells enhances TCR-mediated anti-tumor responses. Related to Fig. 8.

(a-c) WT (+/+) *OTI* CD8^{+} T cells stimulated with N4 peptide (0.5x10^{-6}M) and APCs were transduced with retroviruses (RV) expressing 2A-epitope tagged *6Y-CD3ζ* (*6Y*) or *6F-CD3ζ* (*6F*) before addition to tumor cell cultures. **(a)** Transduced *OTI* T cells were analyzed by FACS for the indicated markers. RV-encoded LNGFR was used to assess transduction efficiency. **(b)**, Transduced *OTI* CD8^{+} T cells were analyzed by immunoblot for the presence of TCR associated 2A-tagged RV-encoded 6Y or 6 F CD3ζ after immunoprecipitation with anti-TCRβ and PAGE to confirm incorporation of transduced ζ chains into the TCR. IP-immunoprecipitated, CL-cell lysate. Data are representative of two independent experiments.(**c**) Plot showing individual tumor measurements related to Fig. 8d.

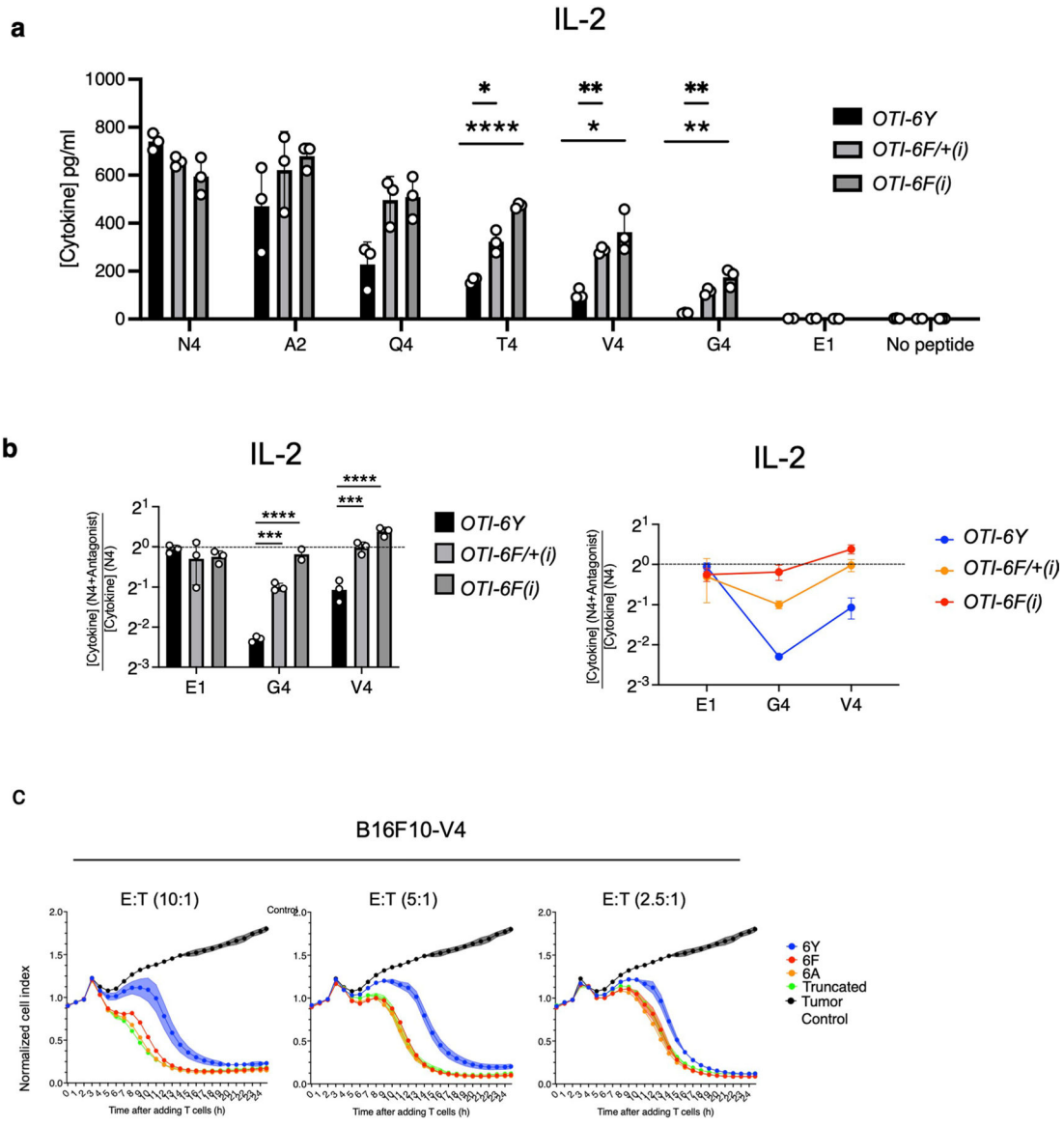

Extended Data Fig. 10 |. *OTI* CD8$^+$ T cells heterozygous for the CD3ζ-6F allele [6F/+(i)] display an intermediate phenotype compared to *OTI-6Y* and *OTI-6F(i)* T cells. Related to Fig. 8.

(a) CD8$^+$ T cells from *OTI 6Y/6Y dLck-Cre-[OTI-6Y], OTI-6Y/+ dLck-Cre + [OTI-6F/+(i)]* and *OTI-6Y/6Y dLck-Cre + [OTI-6F(i)]* mice were co-cultured with APC pulsed with 10^{-8} M of the indicated peptide and accumulation of cytokines was assessed in the culture supernatants at 16 h. N = 3 biological replicates. Data are represented as mean ± SD. Statistical significance determined by two-way ANOVA corrected with Sidak test for multiple comparison. Data are representative of 2 independent experiments. **(b)** Ratio of IL-2 and IFNγ concentrations ('antagonism ratio') for all agonist (N4; 10^{-8} M) / antagonist (V4, G4, E1; 10^{-6} M) combinations. N = 3 biological replicates. Data are represented as mean ± SD. Data are representative of 2 independent experiments. **(c)** Expression of CD3ζ with mutation of the ITAM tyrosines (Y) to phenylalanine (F) or alanine (A) or deletion of the ITAMs (truncated) enhances OTI CD8$^+$ T cell cytotoxic responses. *OTI* (+/+) CD8$^+$ T cells were stimulated with N4 peptide then transduced with retroviruses expressing *6Y*,

6F, *6A* (where all 6 ITAM tyrosines have been mutated to alanine) or a truncated CD3ζ chain lacking the 3 ITAMs. Shown are *in vitro* tumor killing assays at 10:1, 5:1 or 2.5:1 effector-to-target ratios by xCELLigence RTCA (Agilent). *P < 0.05, **P < 0.01, ***P < 0.001, ****P < 0.0001, ns, not significant.

Supplementary Material

Refer to Web version on PubMed Central for supplementary material.

Acknowledgements

We thank L. Samelson (National Cancer Institute (NCI)) and K. Pfeifer (NICHD) for critical reading of the manuscript. This work was supported by the NIH and NCI intramural research programs (Project number: 1ZIAHD001803-29 to P.E.L). Research reported in this publication was supported by the Office of Clinical Research BtB Program Funds-award # 996369 (PEL).

Data availability

All data are available in the main text and supplementary materials. All materials described in this article are available upon request and may require an NIH material transfer agreement. Source data are provided with this paper.

References

1. François P, Voisinne G, Siggia ED, Altan-Bonnet G & Vergassola M Phenotypic model for early T-cell activation displaying sensitivity, specificity, and antagonism. Proc. Natl Acad. Sci. USA 110, E888–E897 (2013). [PubMed: 23431198]
2. Lever M et al. Architecture of a minimal signaling pathway explains the T-cell response to a 1 million-fold variation in antigen affinity and dose. Proc. Natl Acad. Sci. USA 113, E6630–E6638 (2016). [PubMed: 27702900]
3. Altan-Bonnet G & Germain RN Modeling T cell antigen discrimination based on feedback control of digital ERK responses. PLoS Biol 3, e356 (2005). [PubMed: 16231973]
4. Reth M Antigen receptor tail clue. Nature 338, 383–384 (1989). [PubMed: 2927501]
5. Samelson LE & Klausner RD Tyrosine kinases and tyrosine-based activation motifs. Current research on activation via the T cell antigen receptor. J. Biol. Chem 267, 24913–24916 (1992). [PubMed: 1459994]
6. Gaud G, Lesourne R & Love PE Regulatory mechanisms in T cell receptor signalling. Nat. Rev 18, 485–497 (2018).
7. Humphrey MB, Lanier LL & Nakamura MC Role of ITAM-containing adapter proteins and their receptors in the immune system and bone. Immunol. Rev 208, 50–65 (2005). [PubMed: 16313340]
8. Pitcher LA & van Oers NSC T-cell receptor signal transmission: who gives an ITAM? Trends Immunol 24, 554–560 (2003). [PubMed: 14552840]
9. Love PE & Hayes SM ITAM-mediated signaling by the T-cell antigen receptor. Cold Spring Harb. Perspect. Biol 2, a002485 (2010). [PubMed: 20516133]
10. Chan AC, Irving BA & Weiss A New insights into T-cell antigen receptor structure and signal transduction. Curr. Opin. Immunol 4, 246–251 (1992). [PubMed: 1418701]
11. James JR Tuning ITAM multiplicity on T cell receptors can control potency and selectivity to ligand density.Sci. Signal 11, eaan1088 (2018). [PubMed: 29789296]
12. Mukhopadhyay H, Cordoba S-P, Maini PK, van der Merwe PA & Dushek O Systems model of T cell receptor proximal signaling reveals emergent ultrasensitivity. PLoS Comput. Biol 9, e1003004 (2013). [PubMed: 23555234]

13. van Oers NS, Love PE, Shores EW & Weiss A Regulation of TCR signal transduction in murine thymocytes by multiple TCR zeta-chain signaling motifs. J. Immunol 160, 163–170 (1998). [PubMed: 9551968]
14. Hwang S et al. Reduced TCR signaling potential impairs negative selection but does not result in autoimmune disease. J. Exp. Med 209, 1781–1795 (2012). [PubMed: 22945921]
15. Hwang S et al. TCR ITAM multiplicity is required for the generation of follicular helper T-cells. Nat. Commun 6, 6982 (2015). [PubMed: 25959494]
16. Guy CS et al. Distinct TCR signaling pathways drive proliferation and cytokine production in T cells. Nat. Immunol 14, 262–270 (2013). [PubMed: 23377202]
17. Kersh EN, Kersh GJ & Allen PM Partially phosphorylated T cell receptor ζ molecules can inhibit T cell activation. J. Exp. Med 190, 1627–1636 (1999). [PubMed: 10587353]
18. Sloan-Lancaster J, Shaw AS, Rothbard JB & Allen PM Partial T cell signaling: altered phospho-ζ and lack of zap70 recruitment in APL-induced T cell anergy. Cell 79, 913–922 (1994). [PubMed: 8001128]
19. Madrenas J et al. ζ phosphorylation without ZAP-70 activation induced by TCR antagonists or partial agonists. Science 267, 515–518 (1995). [PubMed: 7824949]
20. Kersh EN, Shaw AS & Allen PM Fidelity of T cell activation through multistep T cell receptor ζ phosphorylation. Science 281, 572–575 (1998). [PubMed: 9677202]
21. Reis e Sousa C, Levine EH & Germain RN Partial signaling by $CD8^+$ T cells in response to antagonist ligands. J. Exp. Med 184, 149–157 (1996). [PubMed: 8691128]
22. Pitcher LA, Ohashi PS & van Oers NSC T cell antagonism is functionally uncoupled from the 21- and 23-kDa tyrosine-phosphorylated TCR ζ subunits. J. Immunol 171, 845–852 (2003). [PubMed: 12847253]
23. Ardouin L et al. Crippling of CD3-ζ ITAMs does not impair T cell receptor signaling. Immunity 10, 409–420 (1999). [PubMed: 10229184]
24. Liu H & Vignali DA Differential CD3 ζ phosphorylation is not required for the induction of T cell antagonism by altered peptide ligands. J. Immunol 163, 599–602 (1999). [PubMed: 10395646]
25. Dittel BN, Stefanova I, Germain RN & Janeway CA Jr. Cross-antagonism of a T cell clone expressing two distinct T cell receptors. Immunity 11, 289–298 (1999). [PubMed: 10514007]
26. Stotz SH, Bolliger L, Carbone FR & Palmer E T cell receptor (TCR) antagonism without a negative signal: evidence from T cell hybridomas expressing two independent TCRs. J. Exp. Med 189, 253–264 (1999). [PubMed: 9892608]
27. Daniels MA, Schober SL, Hogquist KA & Jameson SC Cutting edge: a test of the dominant negative signal model for TCR antagonism. J. Immunol 162, 3761–3764 (1999). [PubMed: 10201890]
28. Chandran SS & Klebanoff CA T cell receptor-based cancer immunotherapy: emerging efficacy and pathways of resistance. Immunol. Rev 290, 127–147 (2019). [PubMed: 31355495]
29. June CH, O'Connor RS, Kawalekar OU, Ghassemi S & Milone MC CAR T cell immunotherapy for human cancer. Science 359, 1361–1365 (2018). [PubMed: 29567707]
30. Lo Presti V, Buitenwerf F, van Til NP & Nierkens S Gene augmentation and editing to improve TCR engineered T cell therapy against solid tumors.Vaccines 8, 733 (2020). [PubMed: 33287413]
31. Kochenderfer JN, Yu Z, Frasheri D, Restifo NP & Rosenberg SA Adoptive transfer of syngeneic T cells transduced with a chimeric antigen receptor that recognizes murine CD19 can eradicate lymphoma and normal B cells. Blood 116, 3875–3886 (2010). [PubMed: 20631379]
32. Feucht J et al. Calibration of CAR activation potential directs alternative T cell fates and therapeutic potency. Nat. Med 25, 82–88 (2019). [PubMed: 30559421]
33. Ventura A et al. Restoration of p53 function leads to tumour regression in vivo. Nature 445, 661–665 (2007). [PubMed: 17251932]
34. Zhang DJ et al. Selective expression of the Cre recombinase in late-stage thymocytes using the distal promoter of the *Lck* gene. J. Immunol 174, 6725–6731 (2005). [PubMed: 15905512]
35. Klinger M et al. Thymic OX40 expression discriminates cells undergoing strong responses to selection ligands. J. Immunol 182, 4581–4589 (2009). [PubMed: 19342632]

36. Pitcher LA et al. The CD3 γϵ/δϵ signaling module provides normal T cell functions in the absence of the TCR ζ immunoreceptor tyrosine-based activation motifs. Eur. J. Immunol 35, 3643–3654 (2005). [PubMed: 16259006]
37. Daniels MA et al. Thymic selection threshold defined by compartmentalization of Ras/MAPK signalling. Nature 444, 724–729 (2006). [PubMed: 17086201]
38. Achar SR et al. Universal antigen encoding of T cell activation from high-dimensional cytokine dynamics. Science 376, 880–884 (2022). [PubMed: 35587980]
39. Zehn D, Lee SY & Bevan MJ Complete but curtailed T-cell response to very low-affinity antigen. Nature 458, 211–214 (2009). [PubMed: 19182777]
40. Santori FR et al. Rare, structurally homologous self-peptides promote thymocyte positive selection. Immunity 17, 131–142 (2002). [PubMed: 12196285]
41. Iwata A et al. Quality of TCR signaling determined by differential affinities of enhancers for the composite BATF–IRF4 transcription factor complex. Nat. Immunol 18, 563–572 (2017). [PubMed: 28346410]
42. Selimkhanov J et al. Systems biology. Accurate information transmission through dynamic biochemical signaling networks. Science 346, 1370–1373 (2014). [PubMed: 25504722]
43. Suderman R, Bachman JA, Smith A, Sorger PK & Deeds EJ Fundamental trade-offs between information flow in single cells and cellular populations. Proc. Natl Acad. Sci. USA 114, 5755–5760 (2017). [PubMed: 28500273]
44. François P & Altan-Bonnet G The case for absolute ligand discrimination: modeling information processing and decision by immune T cells. J. Stat. Phys 162, 1130–1152 (2016).
45. Stefanová I et al. TCR ligand discrimination is enforced by competing ERK positive and SHP-1 negative feedback pathways. Nat. Immunol 4, 248–254 (2003). [PubMed: 12577055]
46. van Oers NS, Killeen N & Weiss A ZAP-70 is constitutively associated with tyrosine-phosphorylated TCR ζ in murine thymocytes and lymph node T cells. Immunity 1, 675–685 (1994). [PubMed: 7600293]
47. Stefanová I, Dorfman JR & Germain RN Self-recognition promotes the foreign antigen sensitivity of naive T lymphocytes. Nature 420, 429–434 (2002). [PubMed: 12459785]
48. Plas DR et al. Direct regulation of ZAP-70 by SHP-1 in T cell antigen receptor signaling. Science 272, 1173–1176 (1996). [PubMed: 8638162]
49. François P, Hemery M, Johnson KA & Saunders LN Phenotypic spandrel: absolute discrimination and ligand antagonism. Phys. Biol 13, 066011 (2016). [PubMed: 27922826]
50. Rademaker TJ, Bengio E & François P Attack and defense in cellular decision-making: lessons from machine learning. Phys. Rev 9, 031012 (2019).
51. Stone JD, Harris DT & Kranz DM TCR affinity for p/MHC formed by tumor antigens that are self-proteins: impact on efficacy and toxicity. Curr. Opin. Immunol 33, 16–22 (2015). [PubMed: 25618219]
52. Aleksic M et al. Different affinity windows for virus and cancer-specific T-cell receptors: implications for therapeutic strategies. Eur. J. Immunol 42, 3174–3179 (2012). [PubMed: 22949370]
53. Dave VP Hierarchical role of CD3 chains in thymocyte development. Immunol. Rev 232, 22–33 (2009). [PubMed: 19909353]
54. Hamerman JA & Lanier LL Inhibition of immune responses by ITAM-bearing receptors. Sci. STKE 2006, re1 (2006). [PubMed: 16449667]
55. Snook JP, Soedel AJ, Ekiz HA, O'Connell RM & Williams MA Inhibition of SHP-1 expands the repertoire of antitumor T cells available to respond to immune checkpoint blockade. Cancer Immunol. Res 8, 506–517 (2020). [PubMed: 32075800]
56. Stromnes IM et al. Abrogation of SRC homology region 2 domain-containing phosphatase 1 in tumor-specific T cells improves efficacy of adoptive immunotherapy by enhancing the effector function and accumulation of short-lived effector T cells in vivo. J. Immunol 189, 1812–1825 (2012). [PubMed: 22798667]
57. Lo W-L et al. Slow phosphorylation of a tyrosine residue in LAT optimizes T cell ligand discrimination. Nat. Immunol 20, 1481–1493 (2019). [PubMed: 31611699]

58. Depoil D & Dustin ML Force and affinity in ligand discrimination by the TCR. Trends Immunol 35, 597–603 (2014). [PubMed: 25466309]

59. Klenerman P et al. Cytotoxic T-cell activity antagonized by naturally occurring HIV-1 Gag variants. Nature 369, 403–407 (1994). [PubMed: 7515165]

60. Meier UC et al. Cytotoxic T lymphocyte lysis inhibited by viable HIV mutants. Science 270, 1360–1362 (1995). [PubMed: 7481824]

61. Scheper W et al. Low and variable tumor reactivity of the intratumoral TCR repertoire in human cancers. Nat. Med 25, 89–94 (2019). [PubMed: 30510250]

62. Linette GP et al. Cardiovascular toxicity and titin cross-reactivity of affinity-enhanced T cells in myeloma and melanoma. Blood 122, 863–871 (2013). [PubMed: 23770775]

63. Vardi Y, Ying Z & Zhang C-H Two-sample tests for growth curves under dependent right censoring. Biometrika 88, 949–960 (2001).

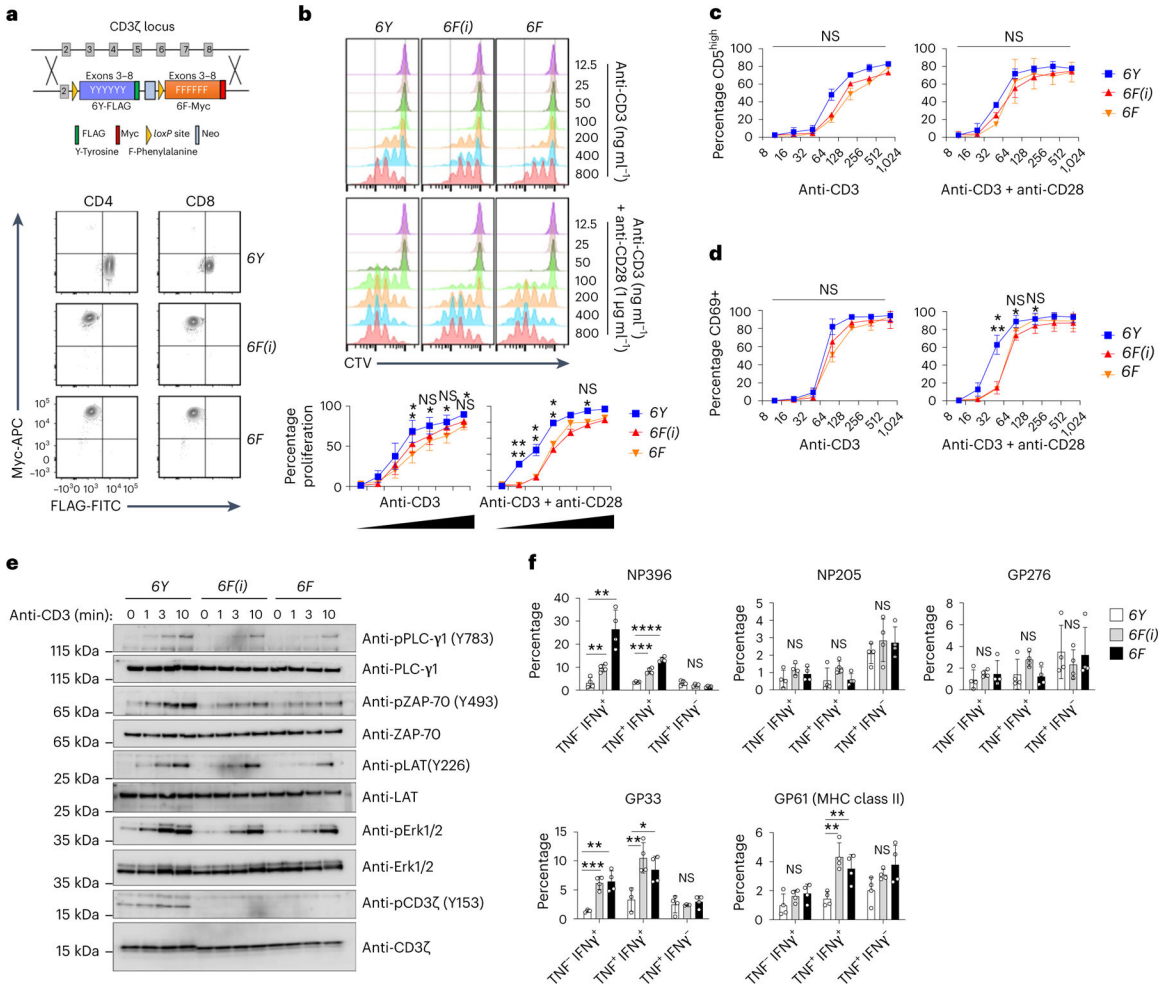

Fig. 1 |. *6F(i)-CD3ζz* T cells exhibit enhanced activation responses to some LCMV ligands.
a, Top, targeting strategy to generate *CD3ζ 6Y-6F* Cre-inducible 'switch' mice. Bottom, expression of 6Y-CD3ζ (FLAG-tagged) and 6F-CD3ζ (Myc-tagged) in $CD4^+$ and $CD8^+$ T cells assessed using intracellular staining. *6Y* (germline *6Y/6Y), 6F* (germline *6F/6F*) and *6F(i)* (*Ert2-Cre*$^+$ *6Y/6Y*) T cells were cultured in vitro with 4-OH tamoxifen (4-OHT) for 2 days before fluorescence-activated cell sorting (FACS) analysis. **b**, Top, proliferation of naive *6Y*, *6F* and tamoxifen-induced *6F(i)* (*Ert2-Cre*) $CD8^+$ T cells stimulated with increasing amounts of plate-bound anti-CD3 alone or in combination with anti-CD28 assessed by cell trace violet (CTV) dilution. Bottom, combined data from three experiments. **c**,**d**, CD5 (**c**) and CD69 (**d**) activation marker expression by tamoxifen-treated naive peripheral $CD8^+$ T cells from *6Y*, *6F* and *6F(i)* (*Ert2-Cre*) mice in response to increasing amounts of anti-CD3 (ng ml^{-1}) alone or in combination with anti-CD28 (1 μg ml^{-1}). For (b-d), statistical comparisons are *6Y* to *6F(i)* (top) or *6Y* to *6F* (bottom). **e**, Activation (phosphorylation) of signaling effectors in naive *6Y, 6F* and *6F(i)* (*dLck-Cre*) $CD8^+$ T cells stimulated with 10 μg ml^{-1} anti-CD3 antibody for the indicated time and analyzed by immunoblot. **f**, *6Y*, *6F* and *6F(i)* (*OX40-Cre*) mice were infected with LCMV Armstrong and spleen T cells were collected and analyzed for cytokine expression 8 days later after peptide restimulation. $n = 4$ for each group. Data were analyzed using a two-tailed, unpaired

t-test and are represented as the mean ± s.e.m. NS, not significant, *$P < 0.05$, **$P < 0.01$, ***$P < 0.001$, ****$P < 0.0001$. The results shown are representative of at least three experiments.

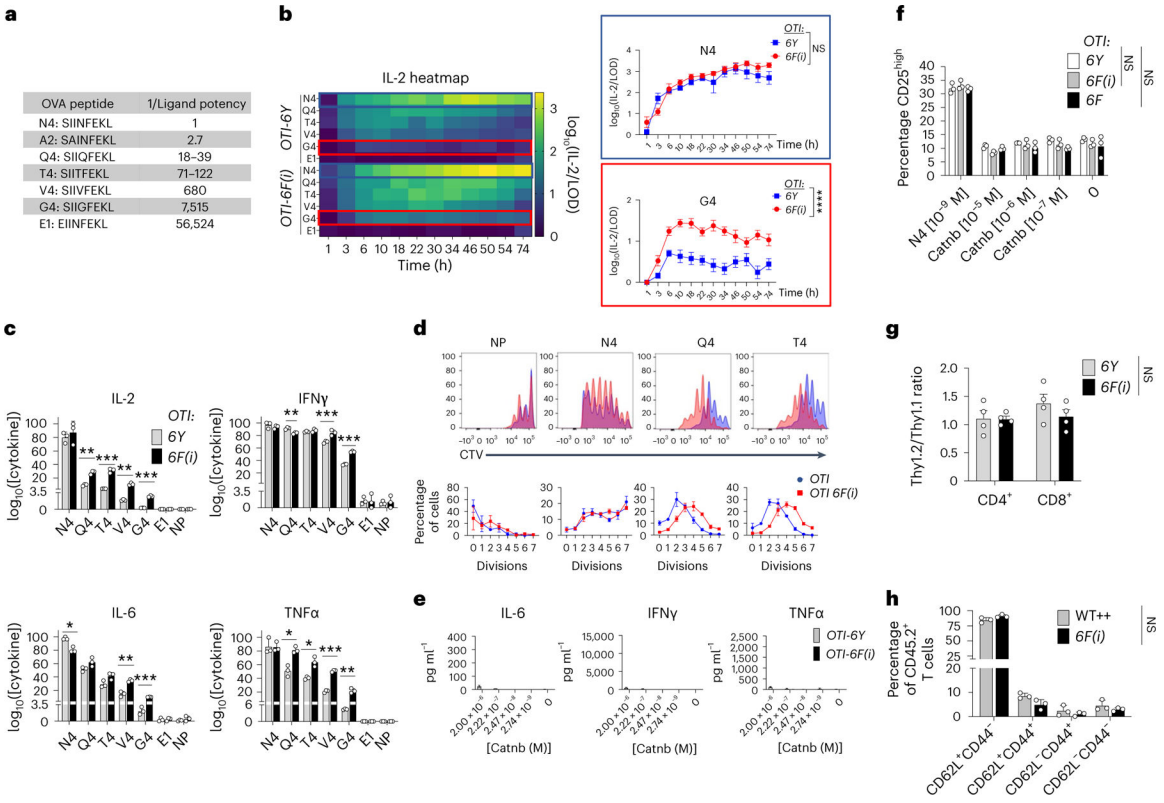

Fig. 2 |. 6F-CD3ζ-expressing T cells have a lower threshold of activation to low-affinity antigens but are not overtly self-reactive.

a, 1/Ligand potency of the different OTI-APLs relative to N4 (refs. 37,39). **b**, Left, heatmap of IL-2 production by *OTI-6Y*, *OTI-6F* or *OTI-6F(i)* (*dLck-Cre*) $CD8^+$ T cells cocultured with APC pulsed with 1 μM of the indicated peptides. Right, time course of IL-2 production after stimulation with N4 or G4 peptides. $n = 6$ biological replicates from two independent experiments. **c**, Cytokine concentrations in the supernatant of stimulated *OTI* $CD8^+$ T cell cultures as detailed in **b** averaged over the entire time course. $n = 3$ biological replicates. In **b**,**c** data are shown as the mean ± s.e.m. and are representative of eight independent experiments. Statistical significance was determined using a two-way analysis of variance (ANOVA) with Šidák correction for multiple comparisons. **d**, In vivo proliferation of CTV-loaded, 4-OH tamoxifen treated *Thy1.1 OTI*$^{+/+}$ and *Thy1.2 OTI-6F(i)* (*Ert2-Cre*) $CD8^+$ T cells coinjected into *Thy1.1/1.2* hosts at a 1:1 ratio followed by injection with (1 μM) peptide-pulsed APCs 24 h later. Spleen and lymph node T cells were analyzed 6 days after injection of APCs. Data shown are representative of two experiments. **e**, Cytokine response of naive *OTI-6Y or OTI-6F(i)* (*dLck-Cre*) $CD8^+$ T cells stimulated with APC pulsed with 1 μM Catnb for 72 h. **f**, *OTI-6Y or OTI-6F(i)* (*dLck-Cre*) $CD8^+$ T cells were preactivated for 6 days with 0.5 μM N4 peptide plus APCs. The graph represents the percentage of $CD25^{high}$ T cells in response to APCs pulsed with the indicated concentration of N4 agonist or Catnb for 48 h. $n = 3$ biological replicates. Data are shown as the mean ± s.d. and are representative of two independent experiments. Statistical significance was determined using a two-way ANOVA with Šidák correction for multiple comparisons. **g**, 4-OH tamoxifen treated *6Y (Thy1.2)* or *6F(i)* (*Ert2-Cre*) *(Thy1.2)* naive T cells were coinjected with *Thy1.1*

(WT+/+) naive T cells at a 1:1 ratio into *Rag2*$^{-/-}$ mice. The *Thy1.2/Thy1.1* ratio of T cells from lymph nodes was analyzed 6 days after injection. $n = 4$ biological replicates. Data are shown as the mean ± s.d. **h**, Bone marrow chimeras were generated with a 1:1 mixture of CD45.1 WT+/+ T-depleted bone marrow cells and either CD45.2 *6F(i)* (*Ert2-Cre*) or CD45.2 WT+/+ T-depleted bone marrow cells. Twelve weeks later, mice received tamoxifen by oral gavage once daily for 5 days and were then euthanized 2 weeks after the last gavage. The graph shows the percentage of naive and memory CD45.2^{+}CD8^{+} T cells from lymph nodes. $n = 3$ biological replicates. The results shown are representative of two experiments. Data are shown as the mean ± s.d. Statistical significance was determined using a two-tailed, unpaired *t*-test. *$P < 0.05$, **$P < 0.01$, ***$P < 0.001$, ****$P < 0.0001$. NP, no peptide.

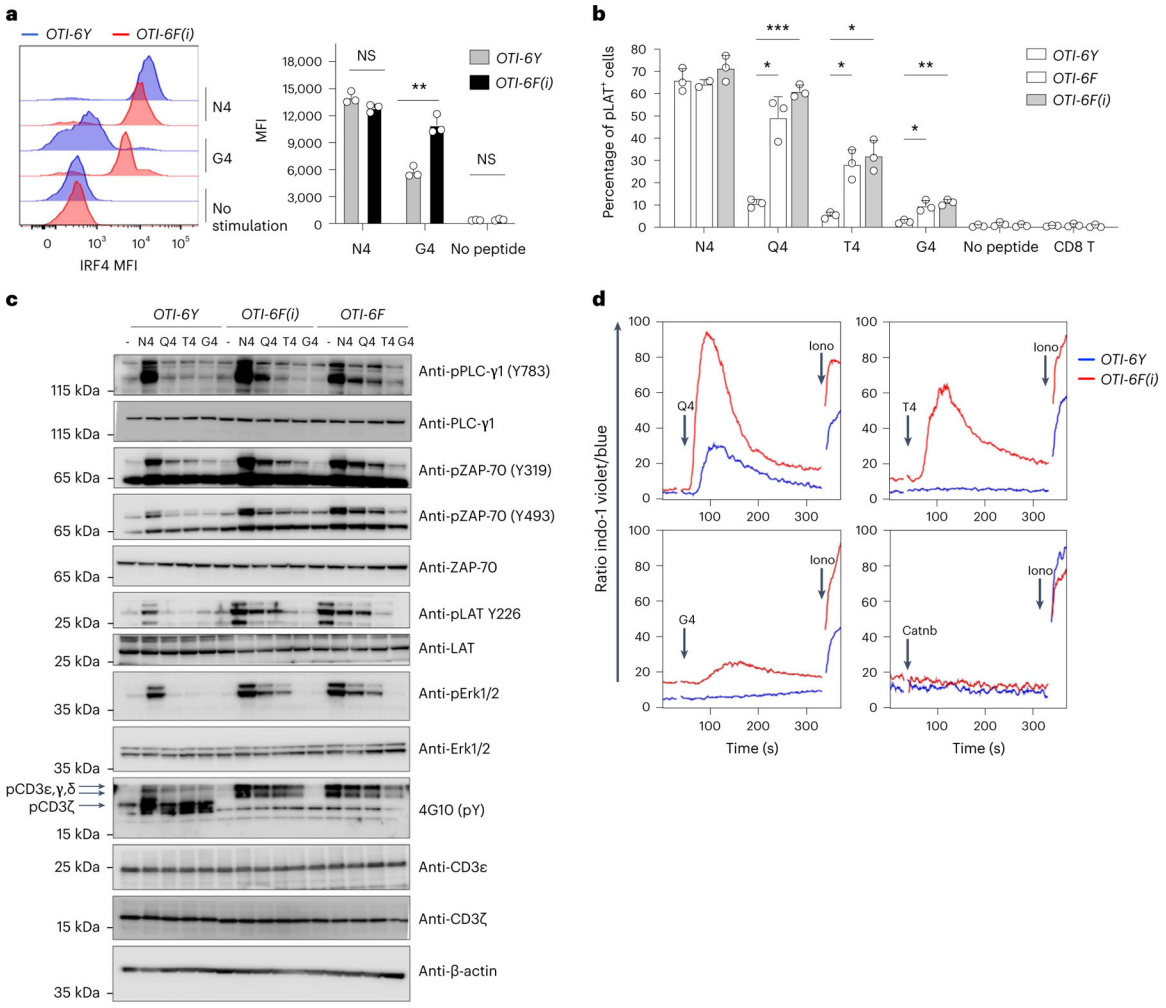

Fig. 3 |. 6F-CD3ζ-expressing T cells display enhanced TCR signaling when stimulated with low-affinity peptides.

a, 4-OH tamoxifen treated *OTI-6Y* and *OTI-6F(i)* (*Ert2-Cre*) CD8$^+$ T cells were stimulated with (1 μM) N4 or G4 peptide-pulsed APCs for 48 h. The FACS plot shows the IRF4 mean fluorescence intensity (MFI) from intracellular staining. Bar graph on right shows data from 3 independent experiments. **b**, 4-OH tamoxifen treated *OT-6Y*, *OT-6F* and *OTI-6Y(i)* (*Ert2-Cre*) CD8$^+$ T cells were stimulated for 2 min with (1 μM) peptide-pulsed APCs. The bar graph shows the percentage of pLAT (pY171)-positive cells from the intracellular staining and FACS analysis. Data are from 3 independent experiments. In **a**,**b**, data are shown as the mean ± s.d. Statistical significance was determined using a two-way ANOVA with Šidák correction for multiple comparisons. **c**, Naive *OTI-6Y and OTI-6F(i)* (*dLck-Cre*) CD8$^+$ T cells were stimulated with the indicated K^b peptide tetramers, lysed and analyzed using polyacrylamide gel electrophoresis (PAGE) and immunoblotting. Data are representative of three independent experiments. **d**, Calcium flux from *OTI-6Y* and *OTI-6F(i)* (*dLck-Cre*) naive CD8$^+$ T cells loaded with indo-1 then stimulated with the indicated K^b peptide tetramers followed by ionomycin. Data are representative of two experiments. Statistical significance was determined using an unpaired *t*-test. $^{**}P < 0.01$.

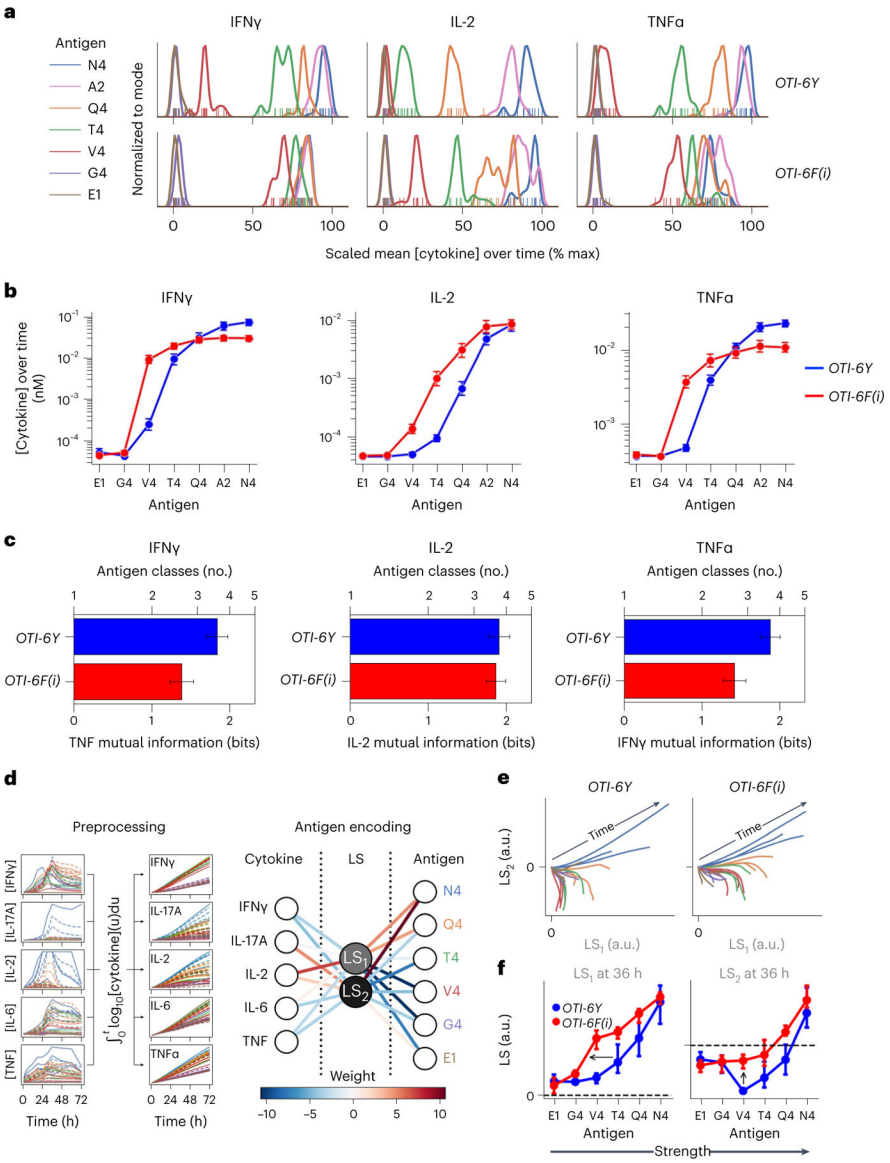

Fig. 4 |. Antigen-stimulated *OTI-6F(i)* CD8$^+$ T cells exhibit reduced ligand discrimination.

a, Averaged distribution of normalized cytokine secretion of 4-OH tamoxifen treated naive *OTI-6Y* or *OTI-6F(i)* (*Ert2-Cre*) CD8$^+$ T cells stimulated with APC + 1 μM antigen of varying affinities. $n = 3$ biological replicates. The data shown are representative of two independent experiments. **b**, Plots of cytokine secretion for IFNγ, IL-2 or TNF averaged over the 72-h time course. $n = 3$ biological replicates. Data are shown as the mean ± s.d. and are representative of at least three independent experiments. **c**, Mutual information (antigen classes) between antigen quality and each secreted cytokine for each genotype. Data are expressed as the MI estimator ± s.d. $n = 3$ biological replicates representative of at least three independent experiments. **d**, Cytokine secretion dynamics of naive *OTI* T cells in response to antigens of six different affinities were preprocessed (left) and then projected into a compressed two-dimensional space (LS_1, LS_2) through the application of the weight matrix obtained from a three-layer neural network trained to predict antigen quality (right)

(*n* = 3 biological replicates). **e**, Time trajectories of LS_1 and LS2 for each antigen in 4-OH tamoxifen treated *OTI-6Y* and *OTI-6F(i)* (*Ert2-Cre*) $CD8^+$ T cells. **f**, LS_1 and LS_2 values at 36 h as a function of antigen affinity. *n* = 3 biological replicates. Data are shown as the mean ± s.d. and are representative of at least three independent experiments.

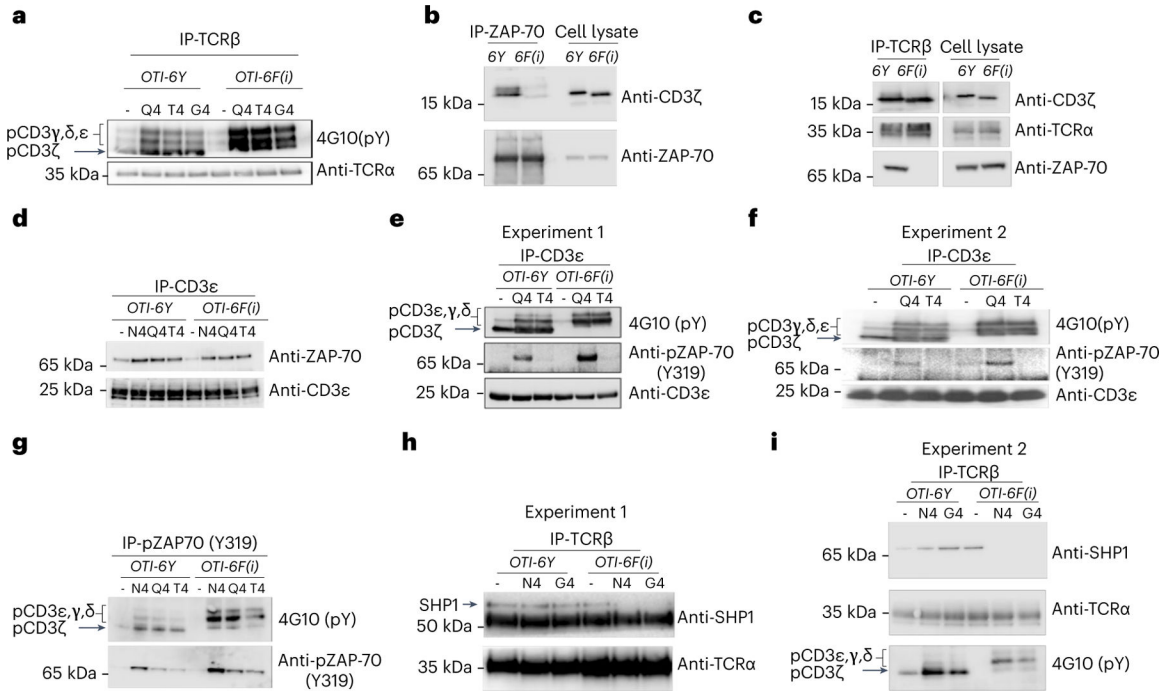

Fig. 5 |. 6F-CD3ζ TCRs do not recruit or retain SHP1 and are associated with more pZAP-70 after pMHC engagement.

OTI-6Y and *OTI-6F(i)* (*dLck-Cre*) naive $CD8^+$ T cells were stimulated for 2 min with the indicated K^b peptide-loaded tetramers (**a**,**d**–**g**) or left unstimulated (**b**,**c**). Cell lysates were incubated with the indicated antibodies; immunoprecipitated proteins or total cell lysates were analyzed using SDS–PAGE and immunoblotted with the indicated blotting antibodies. **a**, *OTI-6Y* and *OTI-6F(i)* $CD8^+$ T cells were stimulated with peptide-loaded tetramers and tyrosine phosphorylated CD3 subunits co-immunoprecipitated with TCRβ were detected by 4G10 blot. **b**, association of ZAP-70 with CD3ζ in unstimulated *OTI-6Y* and *OTI-6F(i)* CD8+ T cells determined by ZAP-70 immunoprecipitation and CD3ζ blotting. **c**, association of ZAP-70 with 6Y or 6F(i) TCRs in unstimulated *OTI-6Y* and *OTI-6F(i)* CD8+ T cells by TCRβ immunoprecipitation and ZAP-70 blotting. **d**, *OTI-6Y* and *OTI-6F(i)* CD8+ T cells were stimulated with peptide-loaded tetramers and ZAP-70 association with the TCR was assessed by CD3ε immunoprecipitation and ZAP-70 blotting. **e**,**f**, *OTI-6Y* and *OTI-6F(i)* CD8+ T cells were stimulated with peptide-loaded tetramers and TCR associated pZAP-70 was detected by CD3ε immunoprecipitation and p(Y319) ZAP-70 blotting. **g**, quantitation of p(319)ZAP-70 and association of pZAP-70 with pCD3 subunits in peptide-loaded tetramer stimulated *OTI-6Y* and *OTI-6F(i)* CD8+ T cells by p(Y319)ZAP-70 immunoprecipitation. **h,i,** *OTI-6Y* and *OTI-6F(i)* CD8+ T cells were stimulated with peptide loaded tetramers and TCR associated SHP1 was evaluated by TCRβ co-immunoprecipitation and SHP1 blotting.

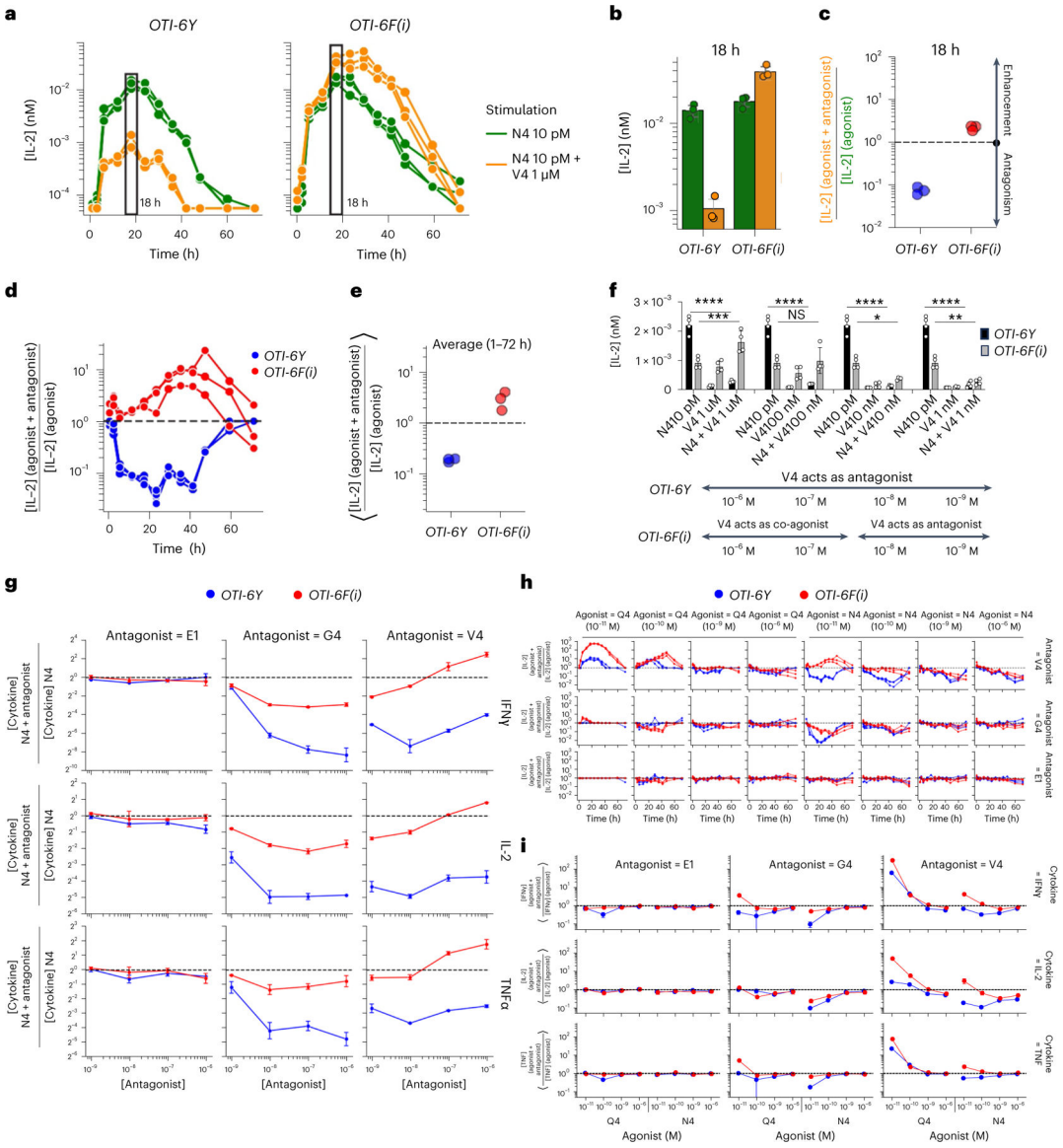

Fig. 6 |. 6F-CD3ζ-expressing T cells have a higher threshold for antagonism.

a, IL-2 secretion dynamics over 72 h for naive *OTI-6Y* or *OTI-6F(i)* (*dLck-Cre*) CD8$^+$ T cells incubated with APCs pulsed with either an agonist alone (N4) or agonist plus antagonist (N4 + V4) at the indicated concentrations (n = 3 biological replicates). **b**, At 18 h, IL-2 levels were markedly lower in *OTI-6Y* T cells stimulated with both N4 and V4 compared to N4 alone, whereas V4 functioned as a co-agonist with N4 for *OTI-6F(i)* T cells. Data are shown as the mean ± s.d. **c**, Antagonism ratio for **b**. Values greater than 1 indicate enhancement of the agonist response by an antagonist ligand, while values smaller than 1 are indicative of antagonism. **d**, Antagonism ratio as a function of time revealed that adding V4 peptide increased IL-2 secretion by N4 peptide-stimulated *OTI-6F(i)* T cells but antagonized IL-2 secretion by N4 peptide-stimulated *OTI-6Y* T cells. **e**, Averaged antagonism ratio over all recorded time points. **f**, CD8$^+$ T cells from *OTI-6Y* and *OTI-6F(i)* (*dLck-Cre*) mice were prestimulated with 10^{-6} M N4 antigen plus APCs for 6 days then restimulated with 10^{-11} M

N4 peptide alone or with different concentrations of V4 peptide plus APC for 24 h. IL-2 in the supernatant was quantified using a cytometric bead array (CBA) assay. $n = 3$ biological replicates. Data are shown as the mean ± s.d. and are representative of at least three independent experiments. *$P < 0.05$, **$P < 0.01$,***$P < 0.001$, ****$P < 0.0001$. Statistical significance was determined using an unpaired *t*-test. **g**, Antagonism ratios for IL-2, IFNγ and TNF calculated by adding different concentrations of E1, G4 or V4 peptides to *OTI-6Y* or *OTI-6F(i)* CD8+ T cells stimulated with 10^{-11} M N4 antigen. $n = 3$ biological replicates. Data are shown as the mean ± s.d. and are representative of two independent experiments. **h**, Kinetics of the ratio of IL-2 concentrations ('antagonism ratio') for the indicated agonist and antagonist combinations ($n = 3$ biological replicates). **i**, Average antagonism plots for different agonist and antagonist combinations and ratios. Antagonist peptide concentrations were 10^{-6} M for all conditions.

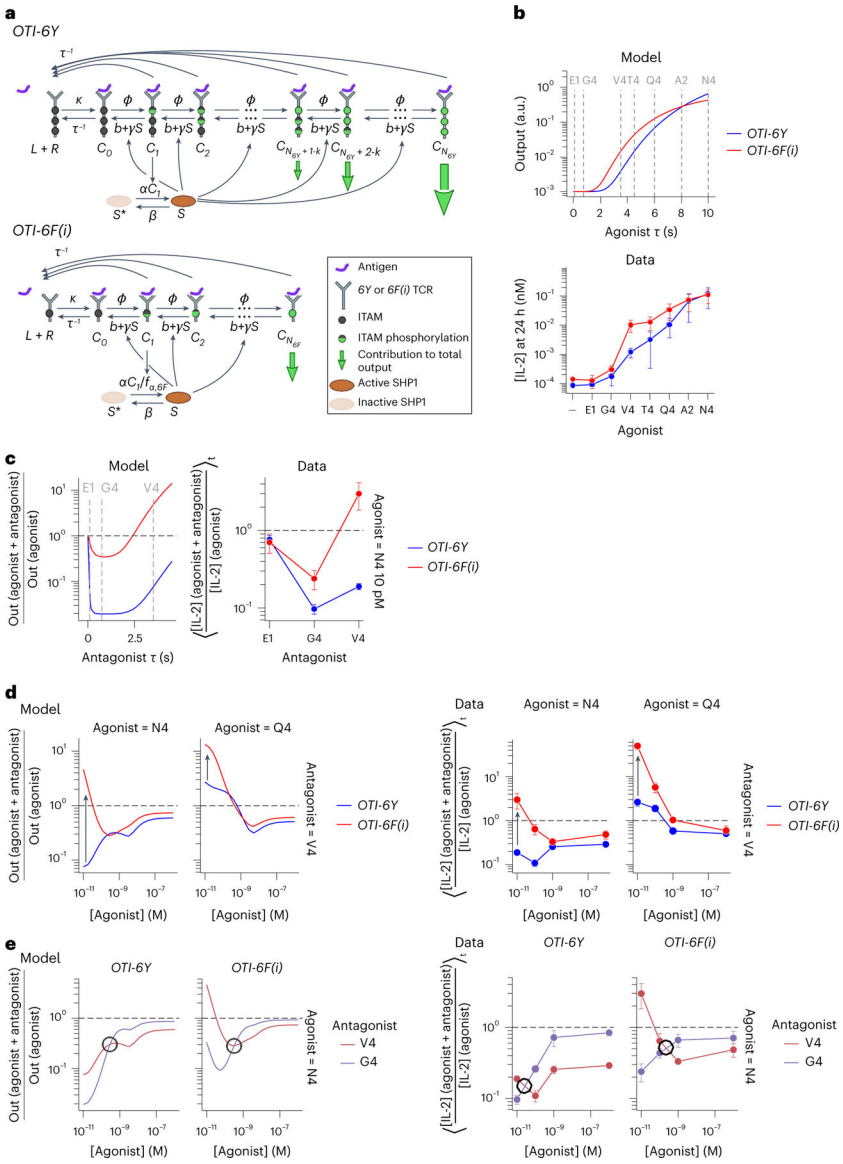

Fig. 7 |. Activation properties of 6F-CD3ζ TCRs are accurately predicted by a new model of KPR with negative feedback.

a, Phenomenological model of TCR activation predicting antagonism, as modified from François et al.[1]. On binding to a ligand (left), the TCR undergoes a series of biochemical modifications (indicated by color changes on ITAMs). Complexes can also unbind, followed by rapid dephosphorylation of ITAMs; thus, the TCR implements a KPR scheme. Complex C_m ($m = 1$) activates the negative feedback realized by the phosphatase SHP1 (S: active, S^*: inactive); SHP1 activation is reduced in *6F(i)* T cells by a factor $f_{\alpha,6F}$ to reflect the experimental observations reported in Fig. 4. To reflect their higher ITAM multiplicity, *6Y* TCRs can undergo N_{6Y} proofreading steps and *6F* TCRs can undergo N_{6F} steps, with $N_{6Y} > N_{6F}$. Moreover, the last $k6Y$ complexes of *6Y* TCRs contribute to the total output (green arrows) compared to only one for *6F(i)*. **b**, Top, model constructed to recapitulate the differences between the responses of *OTI-6Y* and *OTI-6F(i)* T cells to antigens with different affinity for the TCR. Bottom, experimental results as measured by

IL-2 concentration at 24 h in response to different *OTI* peptides. **c**, Comparison of modeled versus experimental results on the degree of antagonism in *OTI-6Y* and *OTI-6F(i)* T cells as a function of antagonist peptide affinity. Both model and experiment show that *OTI-6F(i)* T cells are less susceptible to antagonism than *OTI-6Y* T cells across a range of antagonist affinities, and that there is an optimum range of antagonist affinities needed to maximize an antagonistic response. **d**, Model (left) and experimental results (right) for antagonism as a function of agonist concentration, agonist and genotype (see Fig. 6h,i). Both model and experiment show that *OTI-6F(i)* T cells are antagonized less effectively than *OTI-6Y* T cells. **e**, Model (left) and experimental results (right) for antagonism as a function of agonist concentration, antagonist and genotype for different antagonists (see Fig. 6h,i). Both model and experiment show that the antagonist that produces the largest antagonistic effect changes as the agonist concentration varies. $n = 3$ biological replicates. Data are represented as the mean ± s.d. Data are representative of three independent experiments.

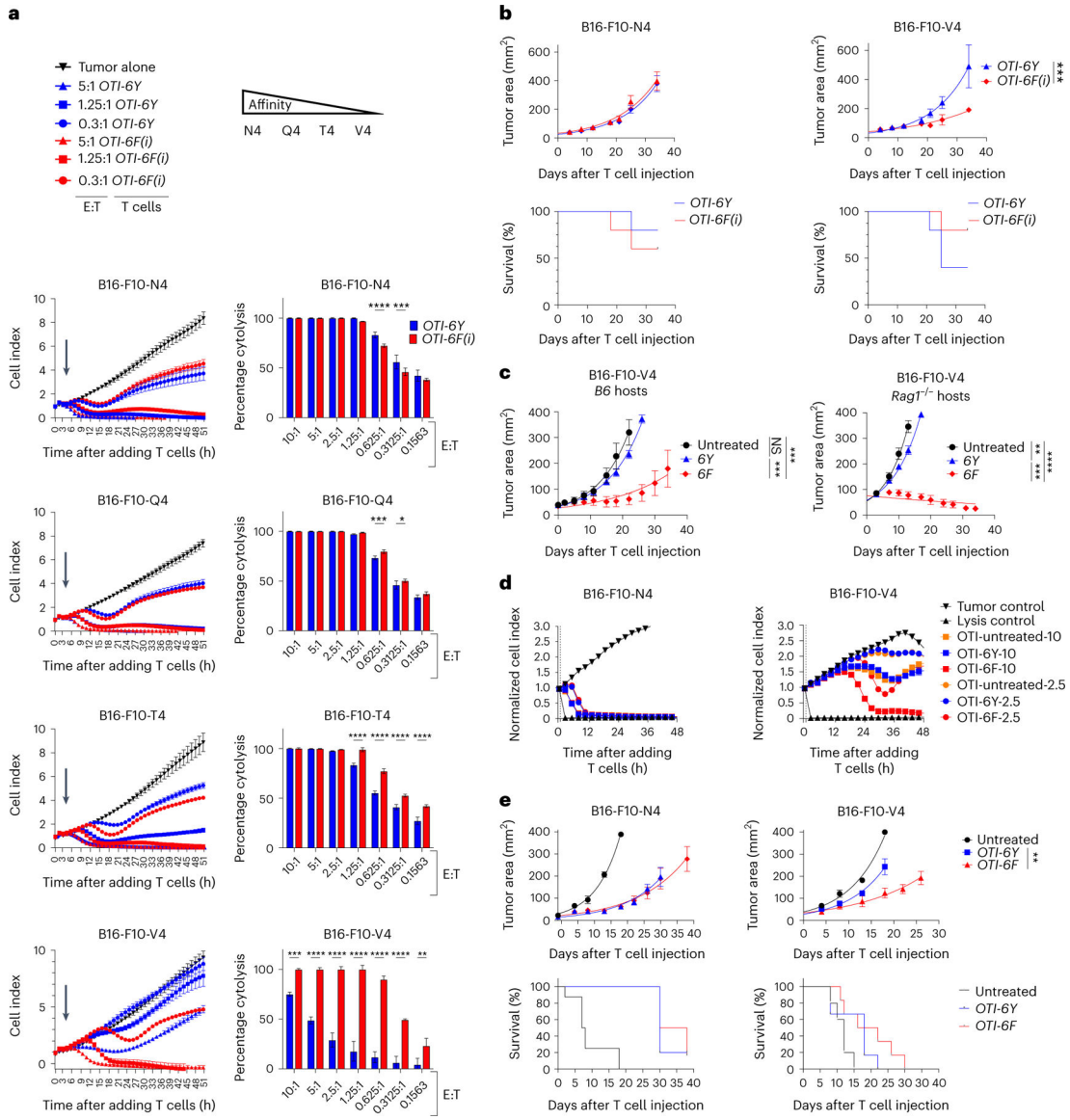

Fig. 8 |. *OTI-6F(i)* CD8$^+$ T cells exhibit higher cytotoxicity toward tumors expressing low-affinity antigens.

a, Left, in vitro tumor killing plots of CD8$^+$ T cells from *OTI-6Y* or *OTI-6F(i)* (*dLck-Cre*) mice at various effector-to-target ratios against B16-F10 melanoma cells expressing N4, Q4, T4 or V4 OVA-APL peptides. The arrow represents the time of T cell addition to the melanoma cell cultures. Right, related killing index (percentage cytolysis) using xCELLigence RTCA for each experiment. Effector-to-target ratios are shown on the *x* axis. *n* = 3 biological replicates. Data are shown as the mean ± s.d. Statistical significance was determined using a two-way ANOVA with Šidák correction for multiple comparisons. Data are representative of three independent experiments. **b**, Top, measurement of the size of B16-F10-N4 or B16-F10-V4 tumors implanted into C57BL/6 mice that were subsequently injected with *OTI-6Y or OTI-6F(i)* (*dLck-Cre*) CD8$^+$ T cells 7 days after melanoma implantation. Bottom, survival plots from the experiment shown above. *n* = 5 biological replicates. Data are representative of three independent experiments. **c**, Experiment similar

to that shown in **b** except that C57BL/6 (left) or *Rag1*$^{-/-}$ (right) mice were injected with *OTI-6Y or OTI-6F* CD8+ T cells. $n = 5$ biological replicates. Results are representative of three experiments. **d**, Experiment similar to that shown in **a** performed with naive *OTI* (+/+) CD8^{+} T cells that were first activated and expanded with anti-CD3 + anti-CD28 antibodies, then left untransduced or transduced with *6Y*-CD3ζ or *6F*-CD3ζ retrovirus. T cells were added to B16-F10-N4 or B16-F10-V4 melanoma cultures at an E:T ratio of 10:1 or 2.5:1; the killing index was recorded by xCELLigence RTCA. One representative of three experiments. **e**, Retroviral transduced T cells as described in **d** were injected into C57BL/6 mice 7 days after B6-F10-N4 or B16-F10-V4 melanoma implantation. Top, measurement of tumor size over time. Bottom, survival plots from the same experiment. $n = 5$ biological replicates. Data are representative of two independent experiments. In **b**,**c**,**e** data are presented as the mean ± s.e.m.; statistical significance was determined with SAS v.9.4 (Methods). *$P < 0.05$, **$P < 0.01$, ***$P < 0.001$, ****$P < 0.0001$.